New Synthesis Framework for the Optimization of Complex Distillation Systems

Piyush B. Shah and Antonis C. Kokossis
Dept. of Process Integration, University of Manchester Institute of Science and Technology, Manchester M60 1QD, U.K.

A new synthesis framework screens and examines complex distillation sequences. Conventional superstructure developments are replaced in favor of a novel representation that assumes the form of a supertask model. The supertask is based on simple tasks that accommodate for basic sequences. Hybrid tasks account for complex columns and sloppy splits. Discrete instances of simple tasks are combined with hybrid transformations to optimize operating conditions. The optimization problem is formulated as a simple MILP problem that is possible to solve to global optimality. The proposed representation can develop different nonconventional and novel designs featuring fully integrated columns, parallel sequences, and multiple-effect columns. The approach is illustrated with several literature and industrial problems. In all cases solutions are reported in the form of nonconventional designs that perform as optimal or near-optimal schemes.

Introduction

Effective screening of separation systems constitutes a critical stage, as engineers need to review and understand trade-offs ahead of detailed modeling and simulation. In the separation, it is often desired to explore the use of complex rather than simple columns, because the complex units reduce mixing losses, use available vapor and liquid more effectively, and improve the separation efficiency (Triantafyllou and Smith, 1992). Despite its recognized potential in energy savings, complex distillation applications are limited due to their difficult and demanding design and synthesis assignment. Synthesis challenges and operability issues that arise from a more complex dynamic behavior have discouraged wider industry acceptance. A prohibitive number of configurations emerge from different allocations of side-rectifiers, side-strippers, prefractionators, and side-draw columns. Such options are difficult to enumerate and assess. The design alternatives increase rapidly and the trade-offs are impossible to assess with an exhaustive (implicit or explicit) enumeration of the options. Although this article does not address dynamics, it presents a simultaneous, systematic, and rigorous approach for the automated development of optimal designs. The approach is computationally inexpensive, reliable, and very efficient to implement. It provides the engineer with a selected set of optimal designs on which further attention to dynamics and operability would yield the final design.

Previous efforts have focused on the development of shortcut methods that were designed to evaluate fixed configurations and initialize simulation models. Stupin and Lockhart (1972) developed the equivalent arrangements of simple columns to represent complex configurations. Several other researchers (Fidkowski and Krolikowski, 1986, 1987, 1990; Glinos and Malone, 1984, 1985; Nikolaides and Malone, 1987, 1988; Carlberg and Westerberg, 1989a,b; Triantafyllou and Smith, 1992) extended knowledge from shortcut models that were available for simple columns to evaluate the performance of complex configurations. Tedder and Rudd (1978) performed a parametric analysis of complex designs and identified optimality regions as functions of the feed composition and the relative volatilities. Glinos and Malone (1988) identified dimensionless parameters and proposed guidelines for the selection of complex distillation schemes. With less emphasis on fixed layouts, thermodynamic methods, proposed by Petlyuk et al. (1965), Kaibel (1987, 1988), and Kaibel

Correspondence concerning this article should be addressed to A. C. Kokossis at this current address: Dept. of Chemical and Process Engineering, University of Surrey, Guildford GU2 5XH, U.K.
Current address of P. B. Shah: AEA Technology-Hyprotech, 707-8th Avenue SW, Suite 800, Calgary, Alberta, Canada T2P 3V3.

et al. (1989), enabled procedures to assess energy efficiency in the integrated separation.

Mathematical programming approaches promote process novelty with the use of superstructure developments. Sargent and Gaminibandara (1976) pioneered a progressive distillation train that Agrawal (1996) later extended with additional connections of vapor–liquid streams to include satellite columns. Christiansen et al. (1997) added more connections between component states to include structures with triangular walls in a single shell. Several researchers [Floudas and Paules, 1988 (regression models); Aggarwal and Floudas, 1992 (regression models); Sargent, 1998; Smith and Pantelides, 1995 (state-equipment-network representation); Bauer and Stichlmair, 1997 (preferred separation with detailed models); Caballero and Grossmann, 1999 (aggregated models); Dunnebier and Pantelides, 1999 (rigorous tray-by-tray models)] developed representations they had to model using mixed-integer nonlinear-programming (MINLP) techniques.

The use of superstructures has helped people to appreciate the large number of options available to review. However, their use fostered complicated interconnections with a large number of variables to account for the design options. More often than not, the optimization technology required to process these models is not addressed as a challenge. Researchers simply assume the technology is available from off-the-self solvers (or other groups) and that the models can be solved and optimized robustly. Consequently, reported designs contain conventional rather than novel and unconventional designs. The development of new mathematical formulations for synthesis problems should not be detached from the optimization technology required to handle these models. Yeomans and Grossman (2000a,b) present some late developments in disjunctive programming and MINLP technology available today.

Papalexandri and Pistikopoulos (1996) propose a representation based on a superstructure of multipurpose heat- and mass-transfer modules. The authors refer to *tasks* as a more general form of a synthesis unit (or block of units). They postulate an even more general (and difficult) problem and propose a detailed modeling framework that relies on the use of MINLP solvers. In contrast to the work by Ismail et al., this article uses the concept of a *task* (Hendry and Hughes, 1972) to reduce rather than enlarge the mathematical model and simplify rather than complicate the optimization. In all cases, the mathematical models are postulated as small MINLP problems one can solve to global optimality.

The new achievements are possible, as the work embraces conceptual and engineering knowledge. In the past conceptual knowledge has been restricted to heuristics and evolutionary approaches, both inappropriate for a systematic search. They typically employ a two-step approach where the best simple sequence is first identified. The sequence is next evolved into complex layouts. Although innovative designs are not excluded, their development is left to coincidence and deprived of a systematic framework. The challenge is to develop systematic procedures that overcome the difficulties encountered with superstructure approaches. This article describes a new synthesis approach that is based on a *supertask* representation. The approach uses simple task and hybrid tasks to conceptualize alternatives. The options include *all* complex column configurations related to side-rectifiers, side-strippers, prefractionators, Petlyuk columns, and side-draw columns. Furthermore, the representation accounts for sequences with sloppy separations and enables us to include optimum pressure limits. The article first describes the multicomponent separation problem that is addressed. The remaining sections formalize the development of supertask and the mathematical models that come from them, all in the form of a mixed-integer linear-programming problem (MILP). The reader is encouraged to relate the supertask representation to the most recent work based on superstructure developments. The number of examples, the quality of the solutions, and the simplicity fostered by the supertask formulation are all worth considering and comparing.

Problem Statement

The approach assumes a number of components to be separated into a predefined set of products. The basic information is given about the components with respect to its physical and critical properties. The objective is to determine the appropriate and cost-effective separation schemes *before detailed simulations*. These include cases of simple columns, thermally coupled side-columns, side-draw columns, prefractionator arrangements, Petlyuk columns, and sloppy splits. The distinctive, and possibly most important, feature of the approach is the way synthesis options are perceived, combined, and conceptualized. In order to address complex systems effectively, this work replaces superstructures with *supertasks*. The building blocks of the latter are not unit-based, but task-based elements.

Without loss of generality, the products are listed in a decreasing order of relative volatility. Unlike methods relying on lumping or pseudocomponents, the multicomponent nature of the products is retained with the use of a recovery matrix. The matrix rows are the components and the matrix columns are the products (normal boiling point increases from left to right). The matrix elements are the fractional recoveries of the components in each product. The representation is applicable to zeotropic systems where the component order does not change with the operating conditions. Table 1 illustrates a matrix of nine components {i-C_4, n-C_4, i-C_5, n-C_5, MCP, CC_6, MCC_6, n-C_8, n-C_9} separated into products A, B, C, and D, as defined in the table. The separation scheme described by the recovery matrix products is apparently different from the one described by the components. For exam-

Table 1. Specifications of Example 1 for the Illustration of Recovery Matrix

			Recovery Fractions in Product			
i	Component	x_i^f	A	B	C	D
1	i-C_4	0.02	1.00			
2	n-C_4	0.04	0.98	0.02		
3	i-C_5	0.05	0.02	0.96	0.02	
4	n-C_5	0.06		0.20	0.80	
5	MCP	0.12			1.00	
6	CC_6	0.10			0.90	0.10
7	MCC_6	0.15			0.08	0.92
8	n-C_8	0.22				1.00
9	n-C_9	0.24				1.00
Product fractions: x_i^P			0.060	0.061	0.271	0.608
Feed flow rate			1,000 kmol/h, saturated liquid			

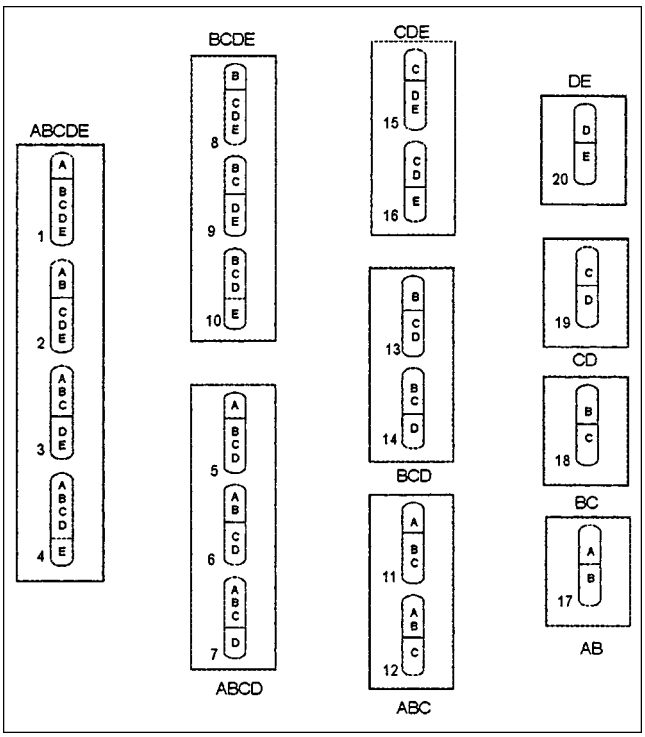

Figure 1. Discrete representation of simple column sequences.

ple, the sharp separation between products B and C (Table 1) corresponds to a nonsharp separation between components i-C_5 and n-C_5 at the specified recoveries.

Tasks were first discussed and presented by Hendry and Hughes (1972), who addressed simple distillation sequencing problems. For an n-component mixture, they identified discrete tasks (T) on the product subgroups (SS) to represent all possible sequences of simple columns (SQ). In a five-product system, the product subgroups are ABCDE, ABCD, BCDE, ABC, BCD, CDE, AB, BC, CD, and DE. The discrete splits on each subgroup yield the tasks given in Figure 1. All simple tasks feature a single feed and two products (a single light and heavy key). Although simple columns are easily represented, it is not possible to render complex arrangements and, unless for a new synthesis framework, the modeling burden of superstructures appears inevitable.

$$SS_n = \frac{(n-1)\cdot n}{2} \tag{1}$$

$$T_n = \frac{(n-1)\cdot n\cdot(n+1)}{6} \tag{2}$$

$$\mathrm{SQ}_n = \frac{[2\cdot(n-1)]!}{n!\cdot(n-1)!} \tag{3}$$

Representation of Complex Distillation Schemes

Apart from simple columns, the synthesis representation is required to embed elementary complex distillation arrangements involving side-columns, side-draw columns, and prefractionators. These complex arrangements are shown in Figure 2. The figure explains two different types of

(1) Side-columns: side-rectifier (Figure 2a), and side-stripper (Figure 2b)

(2) Side-draw columns: vapor side-draw (Figure 2c) and liquid side-draw (Figure 2d)

(3) Prefractionator arrangements: with and without thermal coupling (Figures 2e and 2f). The arrangement shown in Figure 2f is known as a Petlyuk column.

Unlike simple columns, these complex configurations produce more than two products and feature more than a single light- and heavy-key component. A task-based representation of the preceding schemes is accomplished with the ideas of hybrids and sloppy splits.

Hybrid tasks and transformations

Additional tasks are made up of different simple tasks. They are subsequently termed *hybrid* tasks and are defined as ordered combination of simple distillation tasks. The number of tasks in a hybrid defines its *order*. An nth-order hybrid features n splits, n heavy keys, n light keys, and $n+1$ products. A second-order hybrid is shown in Figure 3a. The first light key, LK1, is the light-key component of the lighter split. The second light key, LK2, is the light key of the heavier split. Similarly, first and second heavy keys (HK1 and HK2) are the heavy-key components of the lighter and heavier splits. Figure 3 shows the hybrid formed by the simple distillation tasks AB/CD and C/D. The lighter and heavier splits are B/C and C/D, respectively. Combinations of tasks are only allowed provided the product of one task is a potential feed for the other. In the five-product system, AB/CDE can potentially be combined with A/B, C/DE, or CD/E, but not with A/BC, BC/DE, D/E, and so forth. Products within a hybrid are grouped by hybrid splits. For a second-order hybrid, these groups consist of a light product (LP; components lighter than HK1), a heavy product (HP; components heavier than LK2), and an intermediate product (IP; remaining com-

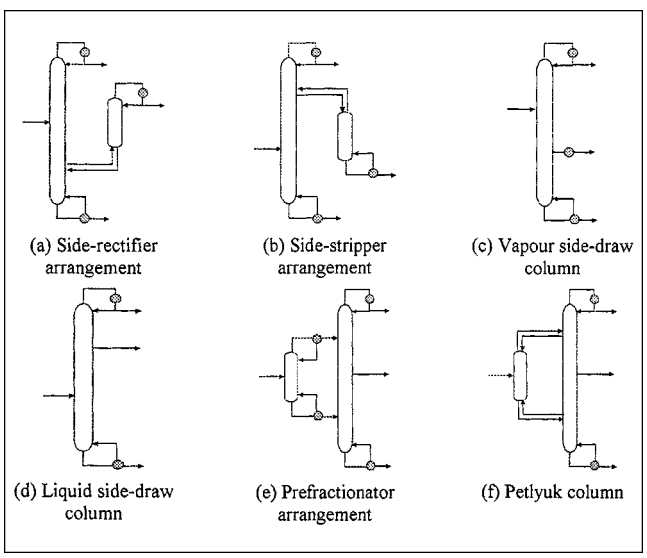

Figure 2. Commonly used complex column arrangements.

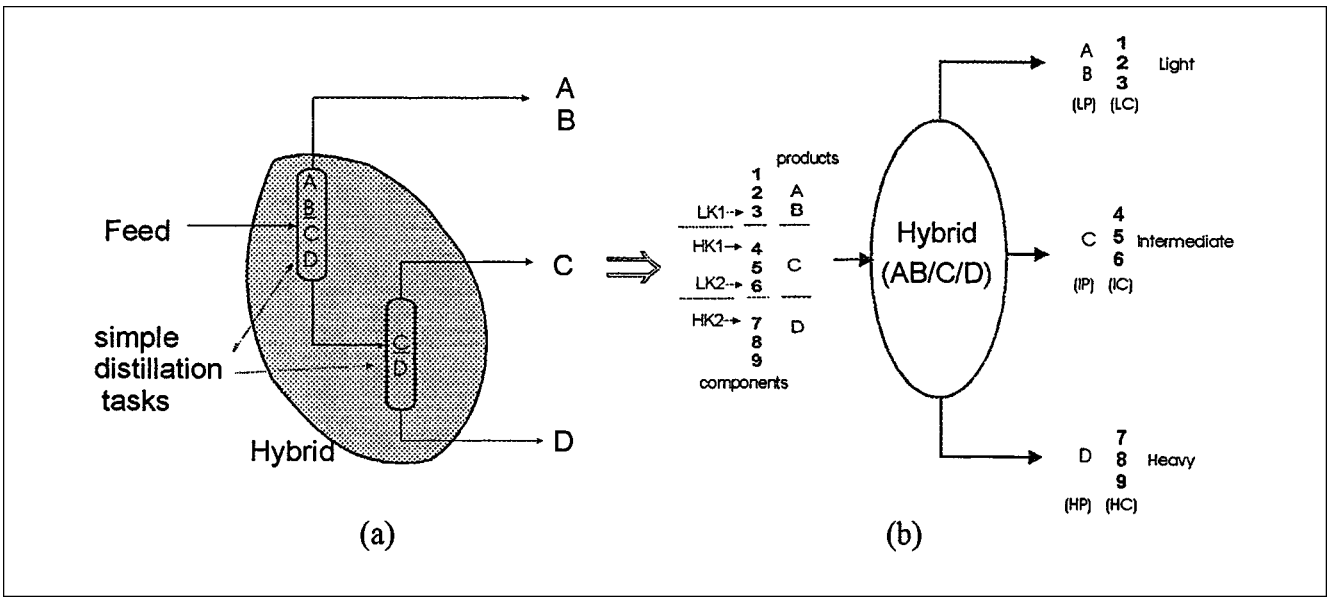

Figure 3. (a) Aggregate of simple tasks; (b) definition of hybrid.

ponents). The components are then clustered into light, intermediate, and heavy components (LCs, ICs, and HCs). Figure 3b illustrates a hybrid AB/C/D of a nine-component feed. The light split is B/C: LK1 = 3 (i-C_5) and HK1 = 4 (n-C_5); the heavy split is C/D: LK2 = 6 (CC_6) and HK2 = 7 (MCC_6).

The possible hybrids, H_n, of the n-product system are given by

$$H_n = \sum_{l=1}^{n-2} \left[l \cdot \sum_{k=1}^{n-l-1} (n-l-k) \right] \tag{4}$$

Although the mapping of the tasks to hybrids is unique, the inverse mapping is not. The sets of map combinations that yield identical hybrids define the *associate sequences* of the hybrid. A second-order hybrid features two associate sequences: the direct sequence *(direct associate)*, and the indirect sequence *(indirect associate)*. The case is illustrated with Figure 4. The hybrid A/B/C can be defined either as a combination of simple tasks A/BC and B/C (direct associate) or AB/C and A/B (indirect associate). Tasks participating in associate sequences define associate tasks of the hybrid. In Figure 4, A/BC, AB/C, A/B, and B/C are the associate tasks of hybrid A/B/C.

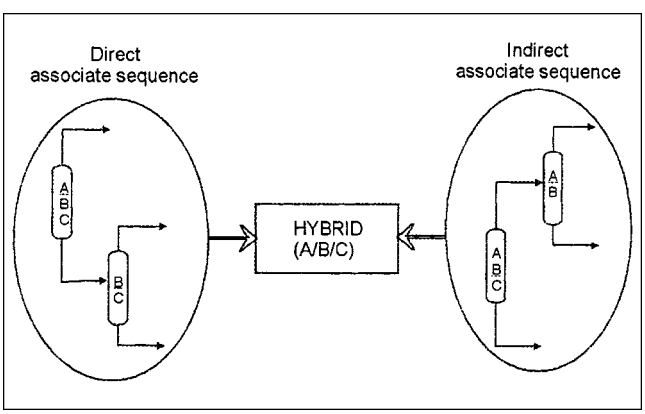

Figure 4. Associate tasks in direct and indirect pairs of hybrid A/B/C.

Transformations of a hybrid are all the complex arrangements represented by the hybrid. The complex arrangements are considered in the context of layouts presented in Figure 2. For a second-order hybrid the direct associate yields:

(1) A single side-column arrangement (side-rectifier);
(2) A single side-draw column (vapor side-draw column);
(3) Two prefractionator arrangements (prefractionator design and Petlyuk column).

For a second-order hybrid the indirect associate yields a single:

(1) Side-column arrangement (side-stripper);
(2) Side-draw column (liquid side-draw column).

The hybrid itself yields all the complex arrangements discussed in Figure 5. Figure 5 illustrates the transformations associated with hybrid B/C/D. The direct associate yields a side-rectifier (sr), a vapor side-draw column (sv), and two prefractionator arrangements (pf and pc). The indirect associate yields a side-stripper (ss) and a liquid side-draw column (sl).

The prefractionation schemes (i.e., prefractionators, Petlyuk columns) are independent of the associate sequences of the hybrid. The associate sequences determine the side-column and the side-draw columns: direct sequences yield side-rectifiers and indirect ones side-strippers. Moreover, the leading tasks of associates represent the leading split of the side-draw columns. On the other hand, the direct associates correspond to vapor side-draw where the light split is the leading split. The indirect associates relate to a liquid side-draw column, with the heavy split as the leading split. Figure 5 illustrates direct and indirect associate sequences, their tasks, and different transformations for the hybrid B/C/D in a five-product system.

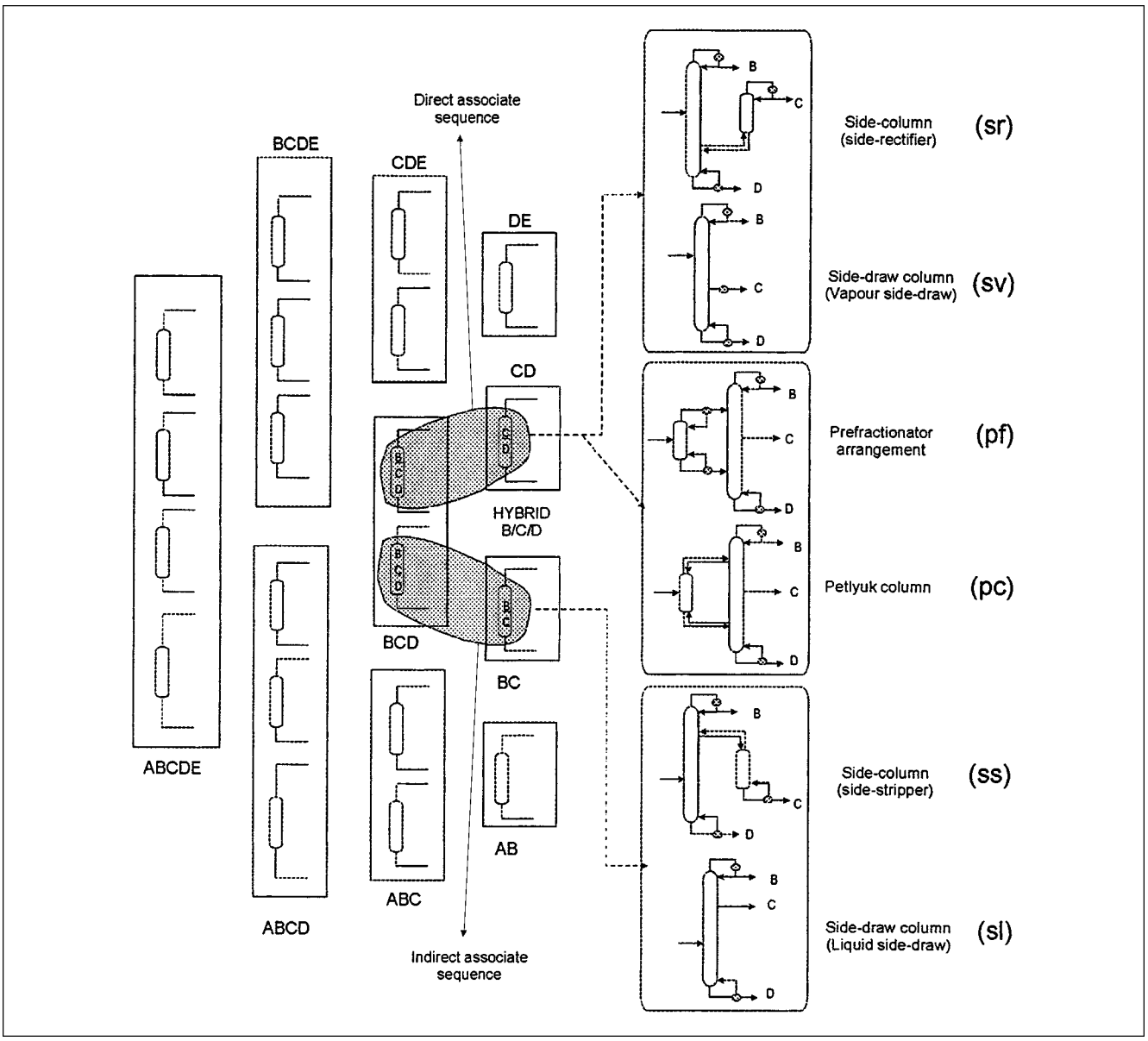

Figure 5. Transformations for hybrid B/C/D in five-product system.

At this point, any new configuration for the separation of three products can be introduced as a hybrid transformation. For example, more operable structures of the Petlyuk column, such as the ones proposed with a unidirectional vapor flow between two thermally coupled shells (Agrawal and Fidkowski, 1998), or partially coupled prefractionator arrangements (Agrawal and Fidkowski, 1998), can be added (and optimized) as new hybrids transformations.

Sloppy split

The sloppy separation improves the separation efficiency by distributing components between the lightest and the heaviest ones. Among the different options for distributing intermediate components (ICs), the maximum efficiency is accomplished by a general sequence of sloppy splits to separate lightest and heaviest products at each stage. Such a sequence is illustrated in Figure 6 for a five-product system. For an n-product system, a hybrid of order $(n-1)$ accommodates a sequence of sloppy splits in the supertask representation. However, it processes each product $(n-1)$ times (for an n-product system) at the expense of energy and column shells. These factors have an adverse effect on the capital and operating costs of the separation system.

To capitalize on the advantages of sloppy split, hybrids of a second order (over n-product systems) are included in arrangements where sloppy splits are followed by sharp separation. These schemes combine the higher separation efficiency of the sloppy splits, while the recurrent processing of products in the downstream sequence is minimized by the sharp

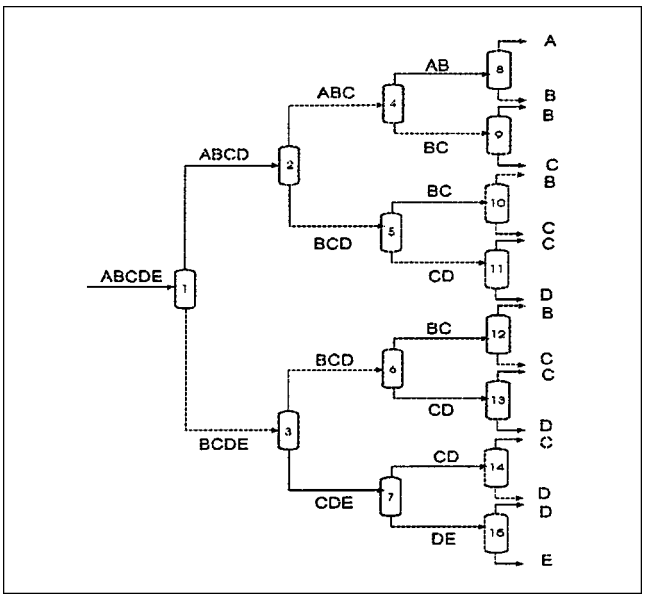

Figure 6. General sequence of sloppy split columns for the five-product system.

separations. The sloppy-split arrangements are introduced as an additional transformation on each hybrid. The sloppy-split transformation consists of a

- Sloppy split between LK1 and HK2 to distribute ICs
- Sharp separation in the downstream columns
- Multiple-feed column to process IP of the hybrid

For a second-order hybrid, the sloppy-split transformation consists of three columns. The first column distributes intermediate components and separates the light product from the heavy product. The downstream columns perform sharp separations. Figure 7 illustrates the case for the hybrid A/BCD/E. Column 1 separates A from E and distributes BCD. The two downstream columns separate A (distillate of Column 2) and E (bottom product of Column 3) from BCD. Sloppy-split columns generate streams of different compositions of intermediate components and provide potential feeds for multiple-feed columns. Indeed, each sloppy split features a unique set of multiple-feed column(s). Because their feed compositions are different, they are treated as different tasks. For an n-product system, the number of distinct multiple-feed columns, MF_n, required to satisfy the sloppy-split arrangements is given by

$$MF_n = \sum_{l=1}^{n-3} l \cdot \frac{(n-l)\cdot(n-l-1)\cdot(n-l-2)}{6} \qquad \forall \quad n \geq 4 \tag{5}$$

Sloppy-split transformations include all $(m-1)$ additional simple tasks for an IP stream with m products. For a second-order hybrid, a sloppy-split arrangement generates two IP streams. Figure 8a illustrates the case for the hybrid B/C/DE. The IP stream carries a single product ($m=1$), so no multiple-feed column(s) are required. Hybrid AB/CD/E (Figure 8b) yields $m=2$, and one two-feed column is required. Hybrid A/BCD/E (Figure 8c) yields $m=3$. The IPs can be separated into two different ways, and two different multiple-feed columns are required.

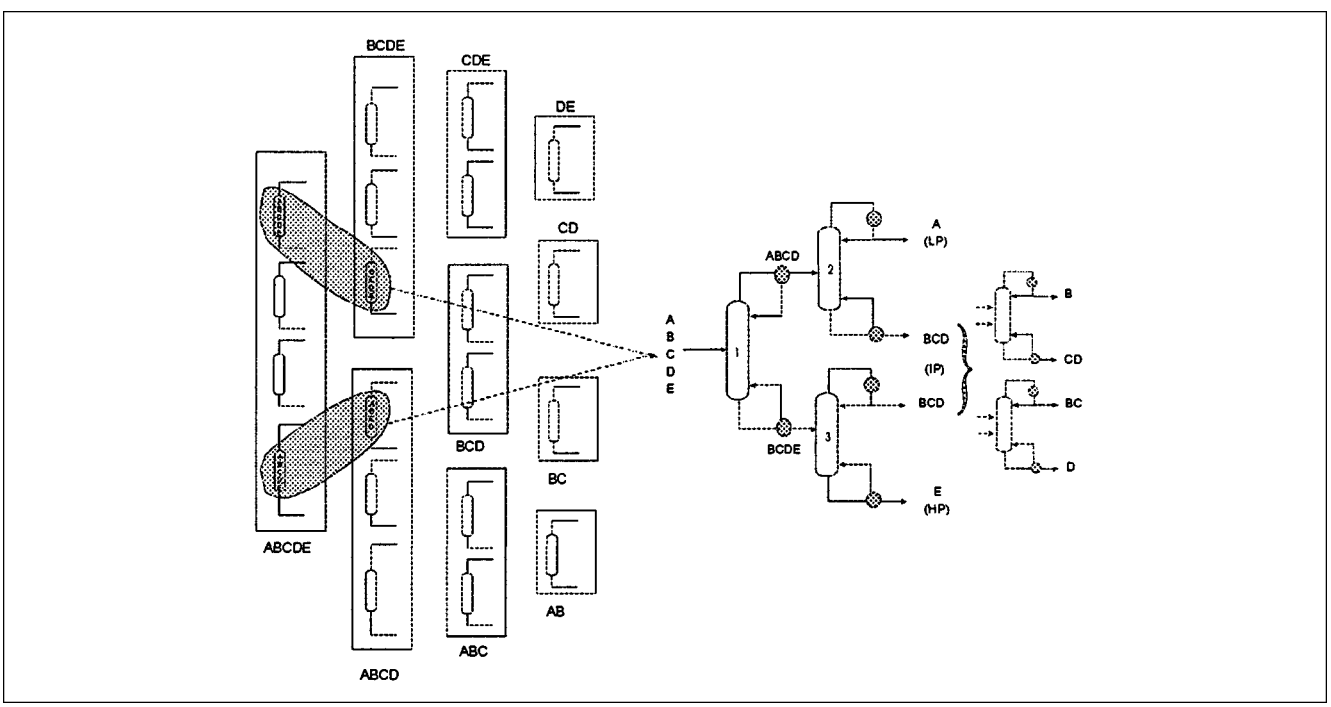

Figure 7. Sloppy split transformation for hybrid A/BCD/E in the five-product system.

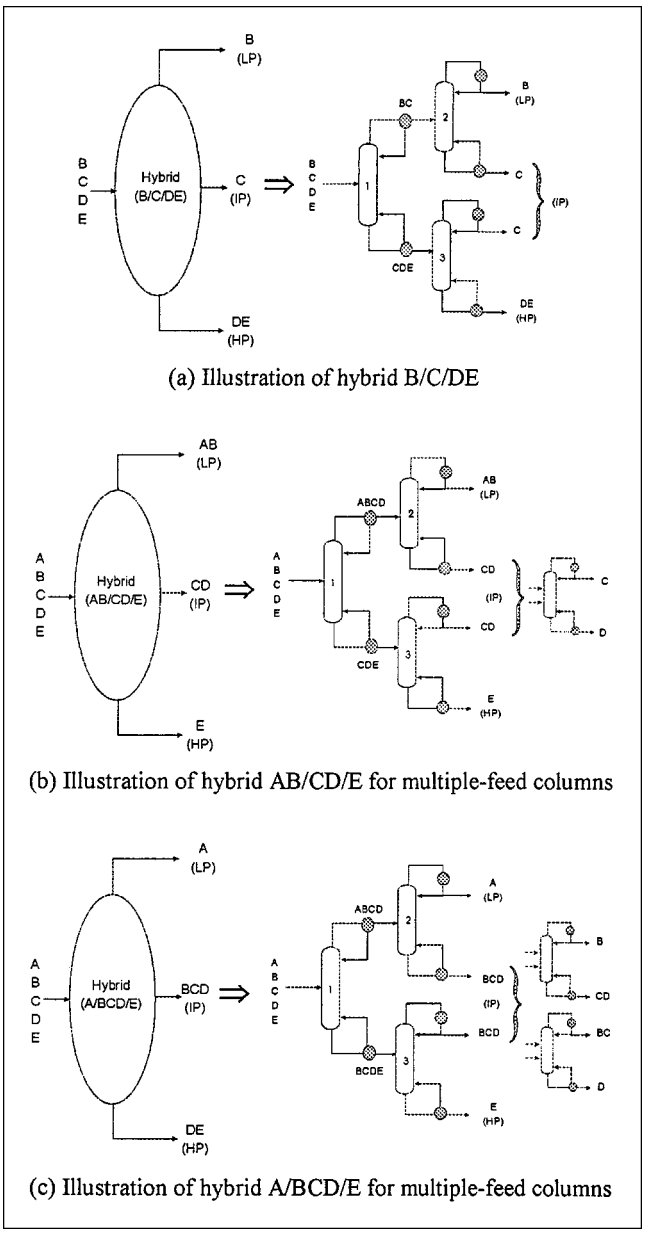

Figure 8. Multiple-feed columns for sloppy split transformation.

Operating conditions

Instances of a task are replicas of the task operating under different conditions. The concept is used to optimize the operating conditions, such as the column pressure, and assumes the development of an operating range and a discretization scheme. Feasible ranges of pressure are identified by the physical properties (such as critical pressure) of the key components (upper limit) and the available utility levels (lower limit). The discretization scheme may be identified either by uniform or based on the available utilities. The modeler can use either a small or large number of discrete levels to capture associated trade-offs. The appropriate numbers depend on the problem. For example, a site with four hot and two cold utilities should require at least six instances. Figure 9 illustrates the development of three discrete instances for the simple task D/E and the side-column transformation (indirect associate) of the hybrid A/B/C. The operation range for D/E is determined by available hot and cold utilities. The pressure range is accordingly discretized to match utility levels. For the side-stripper arrangement, the operation range is defined from the critical properties of the key components and is discretized uniformly.

Supertask representation

The synthesis representation consists of:

(1) Simple tasks to accommodate possible sequences of splits. These are the elements of compartment boxes in Figure 10.

(2) Hybrid tasks to account for complex columns and sloppy-split transformations. These apply (as second-order or higher-order hybrids) to *all* combinations of the elements in 1.

(3) Discrete instances of tasks and hybrid transformations to optimize the operating conditions. These apply to each element of 1 and 2.

The tasks are integrated to create a generic *supertask* representation. Figure 10 illustrates a second-order hybrid B/C/D composed by the associate tasks B/CD and C/D. It also illustrates the transformations attached to the direct associate of the hybrid.

Table 2 summarizes the basic tasks, hybrids, and multiple-feed columns required as a function of the number of products in the feed stream. The number of design options increase rapidly with the number of products in the feed stream, but the number of basic tasks increase slowly and the problem size does not grow larger.

The supertask representation yields different distillation configurations by letting transformations replace the hybrids. This is illustrated in Figure 11. The design of Figure 11a is achieved by letting the prefractionator replace the hybrid A/BCD/E, and the side-rectifier transformation replace hybrid B/C/D. The design of Figure 11b is obtained by letting the sloppy-split transformation replace the hybrid A/BCD/E, and selecting multiple-feed columns to perform the downstream separation. Figure 11c is obtained by letting the side-draw transformation of the direct associate replace the hybrid BC/D/E and select the simple tasks for the remaining separation.

Hybrids with common associate task(s) are the *overlapping hybrids*. They have common key components and products and yield even more complex combinations. Figure 12a illustrates the case where the tasks AB/CDE, CD/E, and A/B are combined to form the two overlapping hybrids AB/CD/E and A/B/CDE. Figure 12b (or 12c) is obtained with a Petlyuk column transformation for AB/CD/E and a side-column transformation for A/B/CDE.

As more tasks are selected on the same operation, parallel sequences are obtained. Figure 13a illustrates the case where the direct and indirect associate sequences of A/BCD/E are simultaneously selected. The sequence produces two separate streams of BCD, but the streams have identical composition and are mixed in downstream separation. Because different transformations of the same hybrid are simultaneously

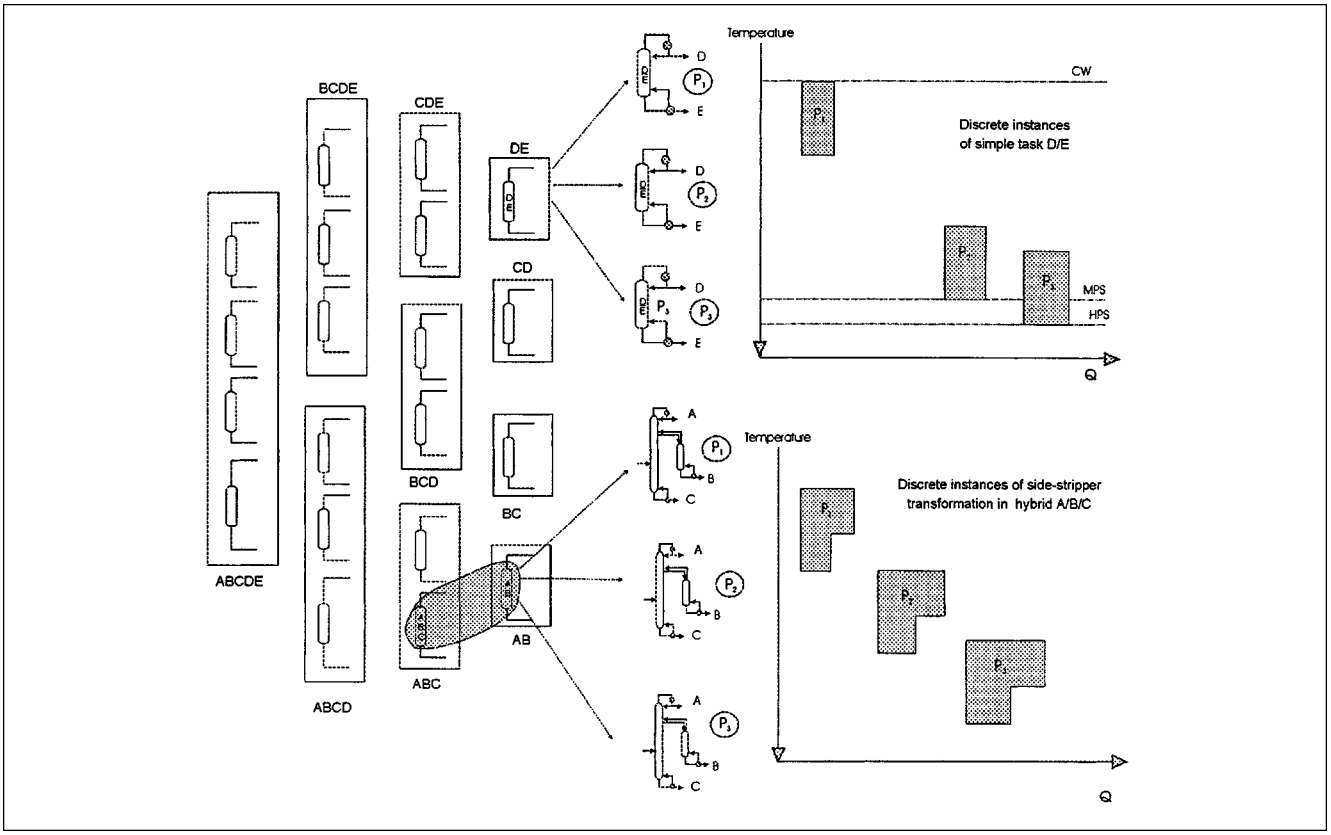

Figure 9. Pressure optimization using discrete instances of basic tasks.

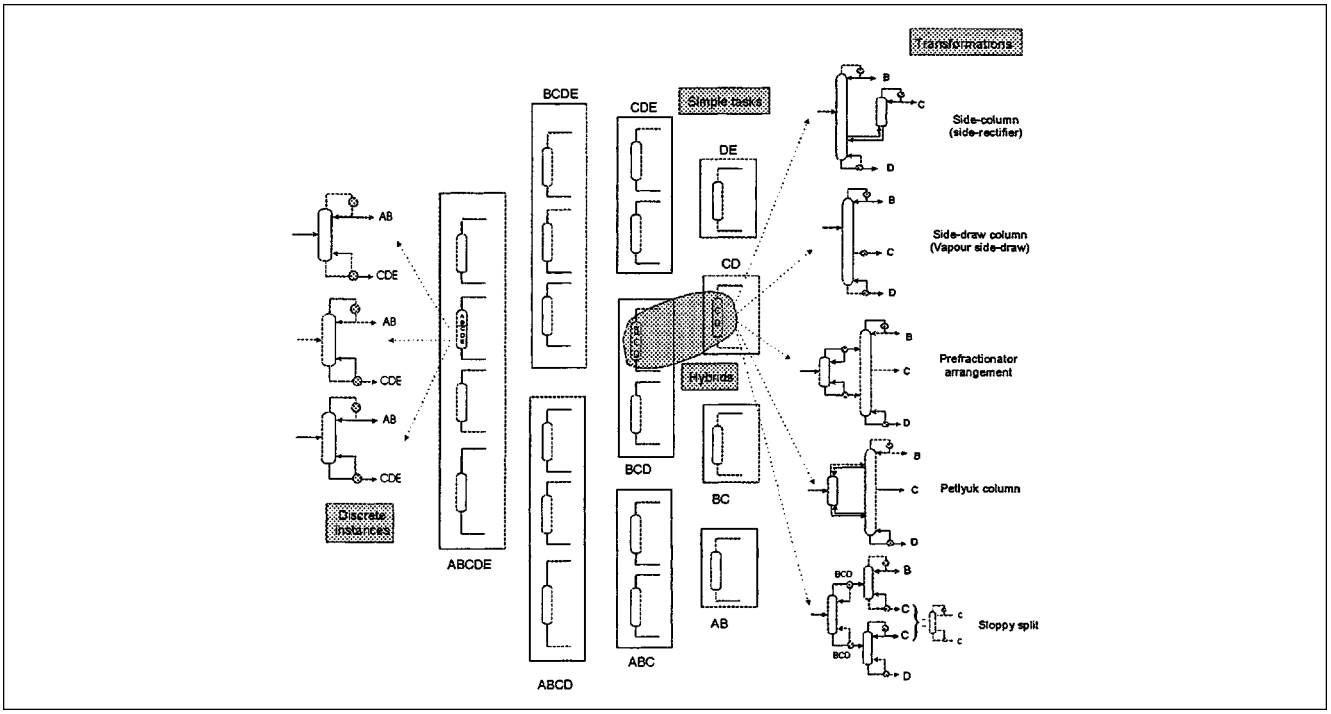

Figure 10. Structure of tasks → supertask representation.

Table 2. Number of Basic Tasks as a Function of Products in the Feed

No. of Products n	No. of Subgroups SS	No. of Simple Tasks T	No. of Hybrids H	No. of Multiple-Feed Column MF
3	3	4	1	—
4	6	10	5	1
5	10	20	15	6
6	15	35	35	21
7	21	56	70	56
8	28	84	126	126
9	36	120	210	252
10	45	165	330	462

selected, many fascinating configurations are developed. Figure 13b illustrates two complex transformations of A/BCD/E selected to operate in parallel. Another parallel sequence is shown in Figure 14a. It employs a direct sequence in parallel with the side-stripper arrangement to separate products A, B, C, and DE. The streams of DE are then mixed before further separation in the simple column. Multiple-effect columns are developed from different discrete instances of the basic tasks. Figure 14b illustrates the case where two different instances of the simple task ABC/DE are combined. Designs of parallel sequences offer novel opportunities in debottlenecking, and retrofit problems of heat integration. The supertask representation is also expandable to other equilibrium-based separation methods (such as extractive distillation).

Modeling of Hybrid Transformations

The synthesis elements of the supertask representation are translated into modeling terms that combine available physical properties with design aspects. At this stage, the work exploits modeling accomplishments from a variety of research groups (Glinos and Malone, 1985; Triantafyllou and Smith, 1992; Koehler et al., 1992), who have separately addressed modeling and simulation challenges of complex distillation configurations. The calculations are used to set up the optimization problem that is formulated in the following section. As an important induction to the details, one should note:

(1) Because of the supertask representation, it is possible to assess and evaluate each task independently and separately from the performance of the upstream or downstream units: the composition and the flow rate of the feed (F). The products streams are known *a priori* and only depend on the separation function of the particular task.

(2) Design and performance calculations can use *any* shortcut or semirigorous or rigorous method, and any property package without influencing constraints and solution strategy of the optimization efforts. By default, the Peng–Robinson equation of state is used to predict the temperatures (such as condenser, reboiler, and so on) and the relative volatilities, and the Underwood–Fenske–Gilliland method (constant relative volatilities and constant molar overflow) is used to predict the vapor traffic and the number of trays.

The approach is not restricted to shortcut models. Rigorous and shortcut models can invariably be used to set up the problem. The list of illustration examples explains the case. It should be noted that the use of rigorous models requires more effort in evaluating the performance of the tasks, but *does not impose any additional computational burden*. These rigorous calculations are of a simulation nature and can be addressed *separately* and prior to the optimization stage. As a result, the optimization effort remains uninfluenced by assumptions of constant relative volatility or the particular property models used for the mixture.

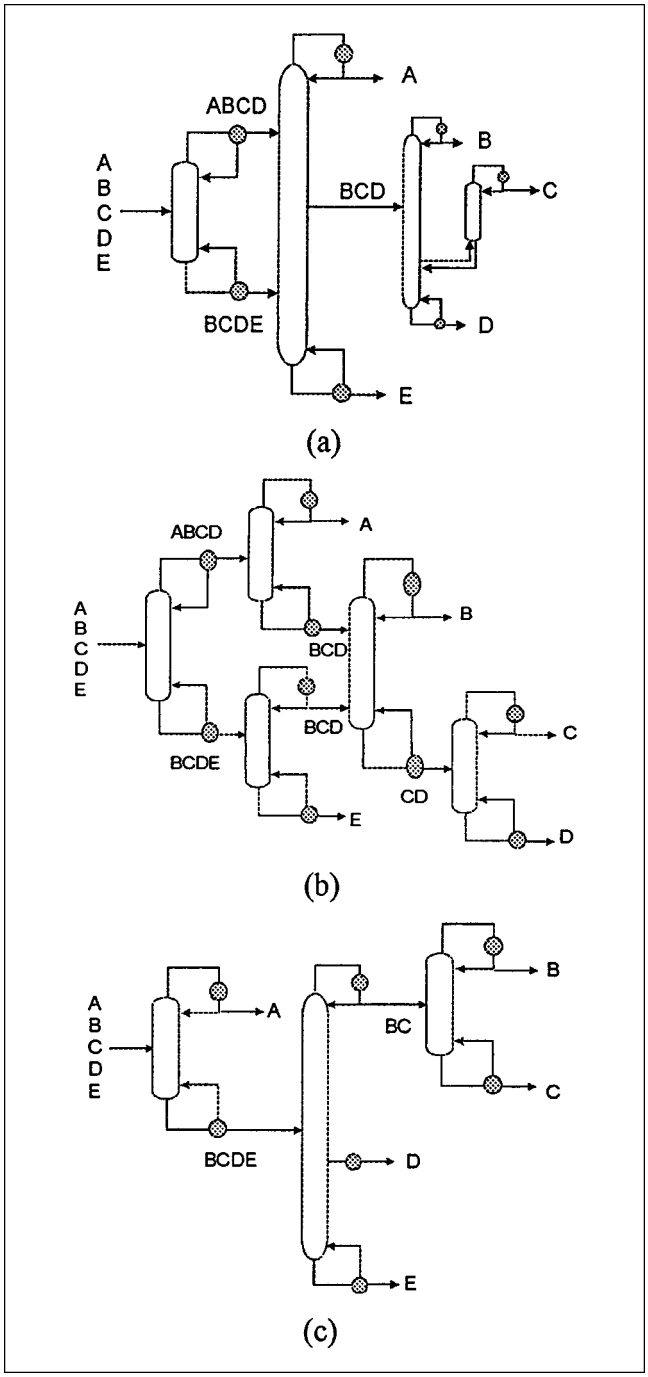

Figure 11. Development of simple and conventional designs from supertask.

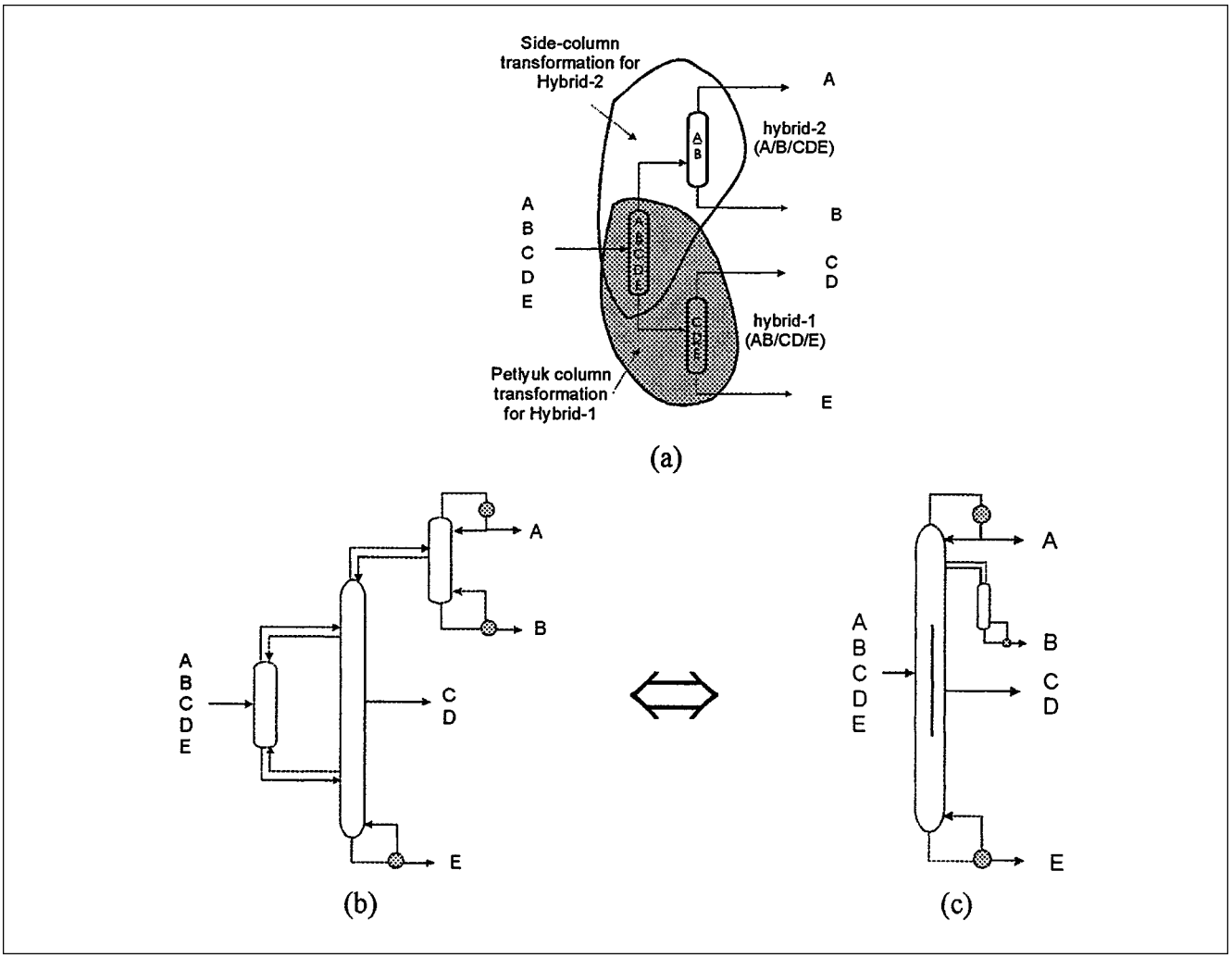

Figure 12. Development of novel designs from overlapping hybrids of supertask.

For each simple task, separate calculations determine the minimum reflux (Underwood method), the minimum number of theoretical stages (Fenske method), the actual number of stages (Gilliland correlation with $R/R_{\min} = 1.1$), the feed-tray location (Kirkbride equation), the condenser and reboiler duties, estimates for the diameter, as well as capital and energy costs (Triantafyllou, 1991). The thermodynamically equivalent arrangements of the various transformations are developed using simple columns, supplementary sections, and hypothetical condensers and/or reboilers (Triantafyllou and Smith, 1992; Glinos and Malone, 1985). For prefractionation-based transformations (that is, prefractionator arrangement, Petlyuk column, and sloppy-split arrangement), the first column fractionates the feed stream to separate the light components from the heavy components; it distributes the intermediate components to minimize its reflux ratio. The recovery of the ICs in the distillate of this column is calculated using the concept of preferred separation (Stichlmair, 1988) and two parts of the Underwood equation. In transformations involving side-draw columns, calculations include the limiting composition of the side-draw (pinch composition under fixed reflux/boilup and the infinite trays in the supplementary section; Glinos and Malone, 1985). If the purity of the side-draw is out of the specified limits, then these configurations are discarded and ignored from the synthesis formulation.

All the calculations are based on the nominal flow rate of the feed stream. Details of the model are presented in the Appendix. For parallel sequences these values are scaled using feed flow-rate fractions. Alternative physical property packages (that is, to replace the Peng-Robinson equation of state) can be embedded without imposing a modeling and computational burden in the optimization. Equally possible are links with new concepts and promising semirigorous or rigorous modeling methods (such as the angle minimization method of Koehler et al., 1992; the geometrical analysis of Bausa et al., 1998).

Mathematical Formulation

The supertask representation of the previous section is formulated as a mathematical model expressed on the basis of

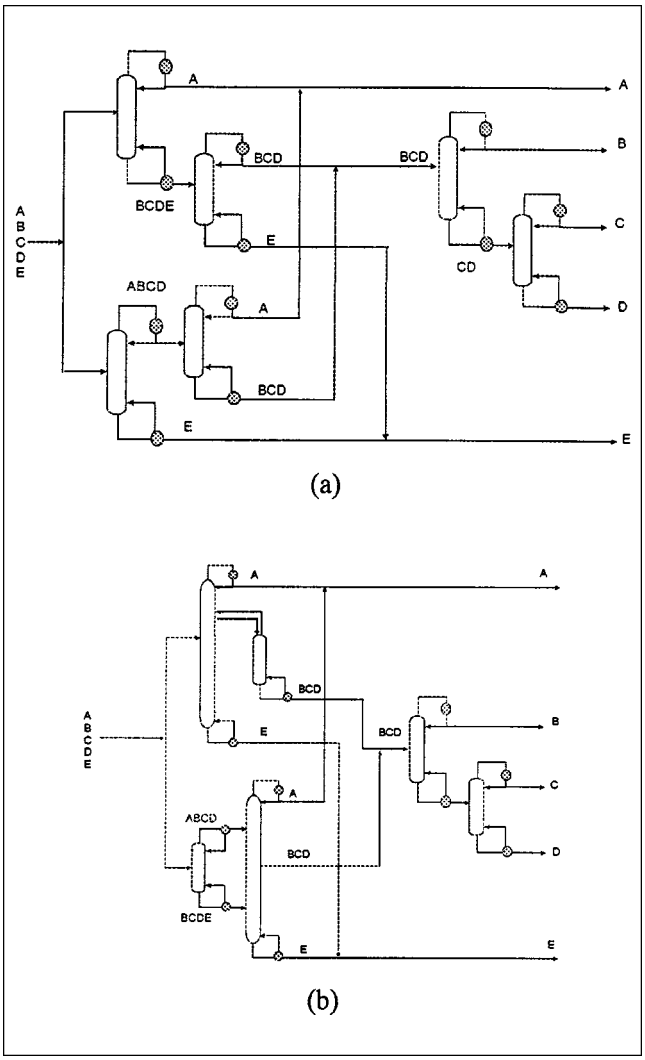

Figure 13. Designs involving parallel sequences.

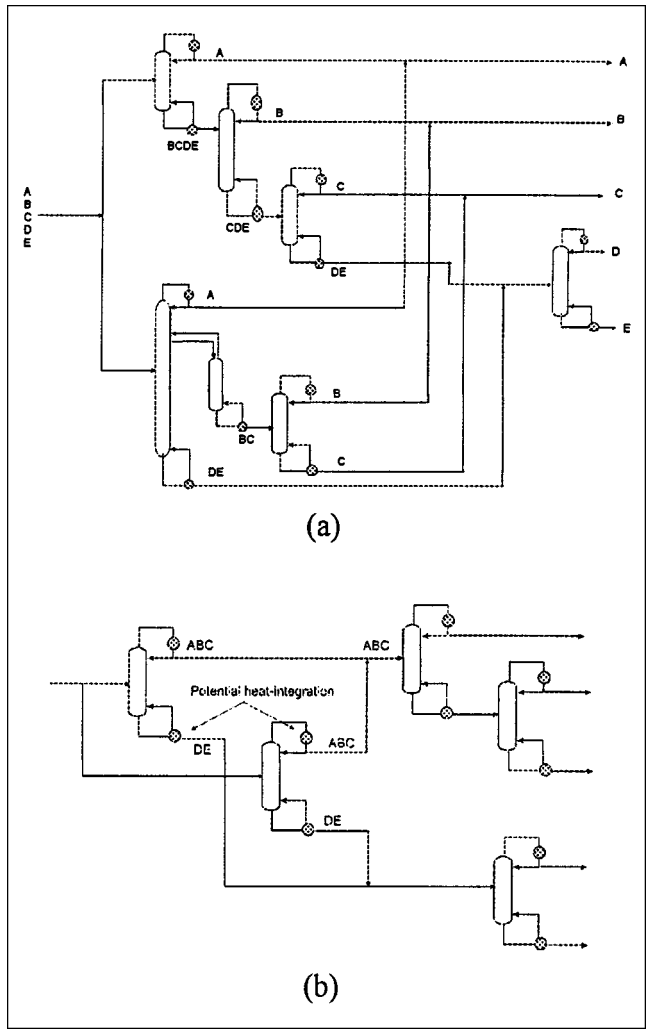

Figure 14. Development of designs involving parallel sequences from supertask.

parameters and variables described as follows:

(1) Sets

$T = \{t | t$ is a simple distillation task$\}$

$H = \{h | h$ is a hybrid task$\}$

$C = \{c | c$ is a transformation of a hybrid task$\} = \{sr, ss, sv, sl, pf, pc, sp\}$

$I = \{i | i$ is a component in the feedstream$\}$

$N = \{n | n$ is a product$\}$

$G = \{g | g$ is a multiple-feed column$\}$

$P = \{p | p$ is a discrete instance$\}$

$M = \{m | m$ is a product subgroup$\}$

The complex transformations *sr* denotes side-rectifier, *ss* a side-stripper, *sv* a vapor side-draw, *sl* a liquid side-draw, *pf* a prefractionator, *pc* a Petlyuk column, and *sp* a sloppy split. Let also,

$C_h = \{u | u \in (h, c)$ with $h \in H$ and $c \in C\}$

$U = T \cup C_h$

Subsets of T include:

$T^{\mathrm{fr}} = \{t | t \in T$ receives fresh feed$\}$

$T^{\mathrm{int}} = \{t | t \in T$ receives intermediate feed$\}$

$T_m^{\mathrm{inp}} = \{t | t \in T^{\mathrm{int}}$ receives stream $m \in M\}$

$T_m^{\mathrm{out}} = \{t | t \in T^{\mathrm{int}}$ produces stream $m \in M\}$

$T_h^{\mathrm{dir}} = \{t | t \in T$ in the direct associate sequence of $h \in H\}$

$T_h^{\mathrm{ind}} = \{t | t \in T$ in the indirect associate sequence of $h \in H\}$

$T_g^{\mathrm{mfd}} = \{t | t \in T$ producing same products with $g \in G\}$

Subsets of C include:

$C^{\mathrm{dir}} = \{c | c \in C$ attached to direct associate sequence$\} = \{sr, sv, pf, pc, sp\}$

$C^{\mathrm{ind}} = \{c | c \in C$ attached to indirect associate sequence$\} = \{ss, sl\}$

Subsets of H include:

$H_t^{\mathrm{asso}} = \{h | h \in H$ attached to associate task $t \in T\}$

Subsets of G include:

$G_h^{\mathrm{slp}} = \{g | g \in G$ attached to sloppy-split transformation of $h \in H\}$

(2) Parameters. The basic parameters of the synthesis problem include:

$\zeta_{m,t}$ = feed fraction yielding stream $m \in M$ in $t \in T$
$E_{u,p}$ = parameter describing the specified objective of $u \in U$ in $p \in P$
$S_{u,p}$ = design discounts in $E_{u,p}$ employing $u \in C_h$, $p \in P$
F_u = nominal feed of $u \in U$
F^{tot} = total feed flow rate
$L_{t,c}^{\text{hyb}}$ = maximum number of $c \in C$ attached to all hybrids of $t \in T$
L_c^{tra} = overall maximum number of transformations, $c \in C$
L_h^{ovl} = maximum transformations of $h \in H$
L_u^{opc} = maximum discrete instances of $u \in U$

(3) Variables. Variables involved in the proposed formulation include:

$Y_{u,p}$ = binary variable for the existence of $u \in U$ in $p \in P$
$f_{t,p}$ = feed flow rate of $t \in T$ in $p \in P$

Constraints of the synthesis problem

Different constraints are imposed on the objective function to establish mass balances, ensure feasibility of the design, and improve the speed of the optimization procedure. They include mass balances around simple tasks

$$F^{\text{tot}} - \sum_{k \in T^{fr}} \sum_{p \in P} f_{k,p} = 0 \tag{6}$$

$$\sum_{t \in T} \left(\zeta_{m,t} \cdot \sum_{p \in P} f_{t,p} \right) - \sum_{k \in T_m^{\text{inp}}} \sum_{p \in P} f_{k,p} = 0 \quad \forall\, m \in M \tag{7}$$

design discounts from the thermal coupling,

$$S_{h,c,p} = \sum_{t \in T_h^{\text{dir}}} E_{t,p} - E_{h,c,p} \qquad \forall\, h \in H,\, c \in C^{\text{dir}} \text{ and } p \in P \tag{8}$$

$$S_{h,c,p} = \sum_{t \in T_h^{\text{ind}}} E_{t,p} - E_{h,c,p} \qquad \forall\, h \in H,\, c \in C^{\text{ind}} \text{ and } p \in P \tag{9}$$

$$S_{g,p} = \sum_{t \in T_g^{\text{mfd}}} E_{t,p} - E_{g,p} \qquad \forall\, g \in G \text{ and } p \in P \tag{10}$$

and constraints relating continuous and binary variables:

$$\sum_{p \in P} f_{t,p} - F_t \cdot \sum_{p \in P} Y_{t,p} \le 0 \qquad \forall\, t \in T \tag{11}$$

Furthermore, logical constraints of binary variables,

$$2 \cdot \sum_{p \in P} Y_{h,c,p} - \sum_{k \in T_h^{\text{dir}}} \sum_{p \in P} Y_{k,p} \le 0 \qquad \forall\, h \in H \text{ and } c \in C^{\text{dir}} \tag{12}$$

$$2 \cdot \sum_{p \in P} Y_{h,c,p} - \sum_{k \in T_h^{\text{ind}}} \sum_{p \in P} Y_{k,p} \le 0 \qquad \forall\, h \in H \text{ and } c \in C^{\text{ind}} \tag{13}$$

$$\sum_{k \in G_h^{\text{sip}}} \sum_{p \in P} Y_{k,p} - \sum_{p \in P} Y_{h,sp,p} = 0 \;\forall\; h \in H \tag{14}$$

$$\sum_{p \in P} Y_{g,p} - \sum_{k \in T_g^{\text{mfd}}} \sum_{p \in P} Y_{k,p} \le 0 \forall\, g \in G \tag{15}$$

contingency constraints,

$$\sum_{p \in P} Y_{t,p} - \sum_{k \in T_m^{\text{out}}} \sum_{p \in P} Y_{k,p} \le 0 \forall t \in T_m^{\text{inp}} \text{ and } m \in M, \tag{16}$$

and constraints on the allowable number of complex columns are included.

$$\sum_{h \in H_t^{\text{asso}}} \sum_{p \in P} Y_{h,c,p} - L_{t,c}^{\text{hyb}} \le 0 \qquad \forall\, t \in T \text{ and } c \in C \tag{17}$$

$$\sum_{c \in C} \sum_{p \in P} Y_{h,c,p} - L_h^{\text{ovl}} \le 0 \qquad \forall\, h \in H \tag{18}$$

$$\sum_{h \in H} \sum_{p \in P} Y_{h,c,p} - L_c^{\text{tra}} \le 0 \qquad \forall\, c \in C \tag{19}$$

$$\sum_{p \in P} Y_{u,p} - L_u^{\text{opc}} \le 0 \qquad \forall\, u \in U \tag{20}$$

Equations 12 and 13 represent constraints that map simple tasks with hybrid transformations. Equation 14 describes the constraint compelling the use of a multiple-feed column whenever the sloppy-split transformation is selected. The constraint to relate the multiple-feed column with a similar simple task is presented by Eq. 15. A set of optional contingency constraints (Eq. 16) improves branching in the optimization. Equation 17 controls the participation of a simple task in attached hybrids and their transformations. Equation 18 checks the number of transformations for each hybrid. Equations 19 and 20 impose bounds on the number of complex configurations and the number of distinct instances for the task. The parameters $L_{t,c}^{\text{hyb}}$ and L_c^{tra} control the network complexity and the extent of thermal coupling. The parameters L_h^{ovl} and L_u^{opc} control the maximum allowable number of branches in the parallel sequence. By setting L_{sv}^{tra} and L_{sl}^{tra} to zero, for example, the side-draw columns can be excluded. Simple sequences are forced by setting $L_{t,c}^{\text{hyb}}$ to zero. The value of L_h^{ovl} and L_u^{opc} are set to one to eliminate parallel sequences. This also provides the necessary control to exclude layouts with temperatures that activate decomposition, coking, or polymerization of components.

It should be noted that the parameters could be set at very large values, essentially enabling even the most complex (and intensely integrated) designs to emerge. The default values of these parameters are set to provide complete freedom in the selection of design. Each simple task can participate in a maximum of three second-order hybrids (one from the feed connection and two from the product connections); hence, the value of $L_{t,c}^{\text{hyb}}$ is set to 3. The separation of feed into n products requires $(n-1)$ simple tasks, and they can form a maximum of $(n-2)$ hybrids; hence, the value of L_c^{tra} is set to $(n-2)$. The values of L_h^{ovl} and L_u^{opc} are set to two to allow a maximum of one parallel branch for each split.

Table 3. Specifications of the Available Hot and Cold Utilities

No.	Type	Temp. (°C)	Cost Index
Hot utilities			
1	Very low-pressure steam (VLP)	90	0.100
2	Low-pressure steam (LPS)	128	0.130
3	Medium-pressure steam (MPS)	174	0.169
4	High-pressure steam (HPS)	196	0.187
5	Very high-pressure steam (VHP)	220	0.241
Cold utilities			
1	Cooling water (CW)	25 to 35	0.017

Note: Data derived from Douglas (1988).

Objective function

The objective function, f^{obj}, draws upon a characteristic quantity, $E_{u,p}$, that can stand for total cost ($Cost_{u,p}^{\text{tot}}$), energy cost ($Cost_{u,p}^{\text{energy}}$), vapor load ($V_{u,p}$), condenser or reboiler duties ($Q_{u,p}^{\text{cond}}$ or $Q_{u,p}^{\text{reb}}$), or any combination of these parameters. The objective assumes the form

$$f^{\text{obj}} = \sum_{t \in T} \sum_{p \in P} E_{t,p} \cdot Y_{t,p} - \sum_{h \in H} \sum_{c \in C} \sum_{p \in P} S_{h,c,p} \cdot Y_{h,c,p} - \sum_{g \in G} \sum_{p \in P} S_{g,p} \cdot Y_{g,p} \quad (21)$$

The proposed formulation results in a mixed integer linear programming (MILP) problem that is solved using OSL/GAMS (Brooke et al., 1988). The optimization simultaneously yields the optimal sequence, the optimal hybrids, and the optimal transformations. The formulation guarantees the global optimality in all cases, as it involves only linear expressions of the continuous variables.

Illustrative Examples

Several examples of nonazeotropic separation systems are presented to illustrate the approach. All products are saturated liquids and the tasks feature total condensers. The operating temperatures and cost indices of all the available utilities are presented in Table 3. In all the cases, a P166 PC is used for the optimization. The values of control parameters and the data on problem size and the computational performance are summarized in Table 4. In all cases, values of parameters L_h^{ovl} and L_u^{opc} are set to 1 (no parallel sequences).

Table 5. Problem Specifications for Example 5C3

I	Component	x_i^f Product NBP (°C)	Recovery Fractions in Product A 77.88	B 82.11	C 96.80	D 107.50	E 117.40
1	Ethanol	0.25	0.98	0.02			
2	*i*-Propanol	0.15	0.01	0.98	0.01		
3	*n*-Propanol	0.35		0.01	0.98	0.01	
4	*i*-Butanol	0.10			0.01	0.98	0.01
5	*n*-Butanol	0.15				0.02	0.98
Product fractions: x_i^P			0.25	0.15	0.35	0.10	0.15
Feed flow rate: F^{tot}			1,000 kmol/h, saturated liquid feed				

Example 5C3: light alcohol separation

The feed stream contains five light alcohols and produces five products. The feed flow rate is 1,000 kmol/h, and Table 5 shows the recovery matrix of the problem (Wankat, 1988). All tasks operate at 1 bar and use cooling water as the only cold utility. The total energy cost is used as the synthesis objective. The selected designs are summarized in Figure 15. Table 6 values the schemes in an order of decreasing performance with Design D1 representing the best simple sequence. Energy savings range from 20% to 25% against this design. The optimization studies four different cases. In each case, the two most promising schemes are selected with Designs A1, B1, and C1 as the optimum and Designs A2, B2, and C2 as the near-optimum.

Case A: Unconstrained Case. Design A1 features a thermally coupled prefractionator for the separation of C and two side-columns for the separation of B and D. This design uses hybrids AB/C/DE (Petlyuk-column transformation), A/B/CDE (side-stripper transformation), and C/D/E (side-rectifier transformation). The choice of hybrids and transformations is illustrated in Figure 16a. Design A2 separates BC from the feed as an intermediate product of the Petlyuk column and uses the side-rectifier for the product D. The design uses hybrids A/BC/DE (Petlyuk-column transformation) and BC/D/E (side-rectifier transformation), as illustrated in Figure 16b.

Case B: No Prefractionation. Design B1 uses a side-rectifier to separate D and employs two side-strippers for the separation of B and C. It uses hybrids ABC/D/E (side-rectifier transformation), AB/C/DE (side-stripper transformations), and A/B/C (side-stripper transformations), as shown in Figure 16c. Design B2 features a side-stripper to separate B and two side-rectifiers to separate C and D. It employs hybrids AB/C/DE (side-rectifier transformation), A/B/CDE (side-

Table 4. Summary of Problem Data and Computational Performance

No.	Example	Controlling Parameters $L_{t,c}^{\text{hyb}}$	L_c^{tra}	L_h^{ovl}	L_u^{opc}	Variables Binary	Continuous	CPU (s)	Results (table)
1	5C3: Case A	3	5	1	1				
2	5C3: Case B	3	0 (*pc*, *pf*, *sp*) 3 (*sr*, *sr*, *sl*, *sv*)	1	1	131	20	51	6
3	5C3: Case C	1	5	1	1				
4	5C3: Case D	0	0	1	1				
5	4R1	3	4	1	1	138	30	68	10
6	6C1	3	6	1	1	301	35	130	13
7	8C1	1	8	1	1	1,092	84	387	15

Design	Energy Cost	Layout	Column	Trays	Temp.(°C) Top/Bottom	Duty (GJ/h) Top/Bottom
A1	29.9	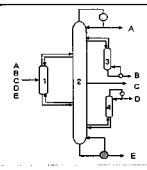	1	7	84.0/104.3	---/---
			2	225	77.2/117.0	-178.0/82.0
			3	49	---/81.0	---/122.0
			4	22	107.0/---	-27.2/---
Columns 1,2: pc for AB/C/DE; 2,3: ss for A/B/CDE; 2,4: sr for C/D/E						
A2	30.4	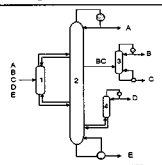	1	6	83.0/103.2	---/---
			2	248	77.2/117.0	-148.0/172.0
			3	22	107.0/---	-26.7/---
			4	42	81.0/96.0	-34.6/35.6
Columns 1,2: pc for A/BC/DE; 2,4: sr for BC/D/E; 3: B/C						
B1	30.8	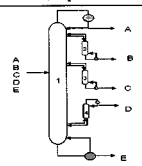	1	212	77.2/117.0	-187.0/56.0
			2	49	---/81.0	---/131.2
			3	25	---/96.0	---/28.4
			4	22	107.0/---	-26.1/---
Columns 1,4: sr for ABC/D/E; 1,3: ss for AB/C/DE; 1,2: ss for A/B/C						
B2	30.9	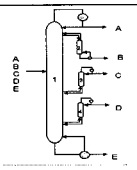	1	189	77.2/117.0	-138.0/87.3
			2	48	---/81.0	---/122.0
			3	44	96.0/---	-43.5/---
			4	22	107.0/---	-27.2/---
Columns 1,3: sr for AB/C/DE; 1,2: ss for A/B/CDE; 1,4: sr for C/D/E						
C1	31.4	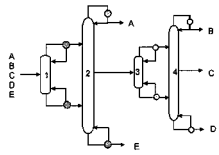	1	5	86.4/103.8	-14.2/14.9
			2	207	77.2/117.0	-142.6/134.6
			3	7	89.1/99.3	-17.7/18.0
			4	104	81.2/107.0	-54.3/43.9
Columns 1,2: pf for A/BCD/E; 3,4: pf for B/C/D						
C2	39.9	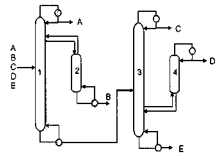	1	140	77.2/103.0	-175.8/57.3
			2	49	---/81.0	---/122.0
			3	104	96.0/117.0	-61.7/93.1
			4	22	107.0/---	-27.2/---
Columns 1,2: ss for A/B/CDE; 3,4: sr for C/D/E						
D1	40.6	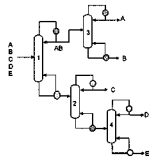	1	42	78.5/101.4	-54.1/57.4
			2	63	96.0/112.0	-61.7/62.8
			3	147	77.2/81.0	-119.8/123.8
			4	62	107.0/117.0	-31.2/33.1
Columns 1: AB/CDE; 2:C/DE; 3: A/B; 4: D/E						

Figure 15. Promising designs for Example 5C3.

stripper transformation), and C/D/E (side-rectifier transformation), as illustrated in Figure 16d. Designs A1, A2, B1, and B2 are achieved by superimposing selected transformations on overlapping hybrids simultaneously. Figure 16 represents associate sequences, hybrids, and corresponding transformations for the development of these novel designs.

Case C: No Transformations of Overlapping Hybrids. The control on thermal coupling is achieved by disallowing the simultaneous selection of different transformations for the overlapping hybrids. Design C1 features two prefractionators that first separates all the intermediate products (that is, B, C, and D) from the feed, and the latter performs the downstream separation. It uses two nonoverlapping hybrids A/BCD/E and B/C/D with prefractionator transformation. Design C2 features a side-stripper for the first column to separate B and a side-rectifier for the second column to separate D. It uses hybrids A/B/CDE (side-stripper transformation) and C/D/E (side-rectifier transformation).

Table 6. Comparison with the Simulation Results for Example 5C3

No.	Design	Energy Cost (%)	Simulation Energy Cost (%)
1	Design A1	74	76
2	Design A2	75	77
3	Design B1	76	77
4	Design B2	76	78
5	Design C1	77	79
6	Design C2	98	85
7	Design D1	100	100

Case D: No Complex Columns. Design D1 represents the best sequence of simple columns that performs the balanced separation first and reserves the difficult (A/B) split for the end. The cost of this simple column sequence is 6,156 k$/y, and this value is used as the basis for the comparison of the remaining designs. The heuristic approach by Wankat (1988) and the fuzzy-logic approach by Flowers et al. (1994) have reported the same simple sequence as the best design.

All tasks operate at the same pressure, hence the adverse effects from thermal coupling are minimal. Consequently, extensive thermal coupling is observed in the designs. There is a strong preference for prefractionators and Petlyuk types of designs due to the large amount of C in the feed (35%). Instead, B and D appear in small quantities and are recovered through side-column arrangements.

The promising designs are simulated using a rigorous model of commercial software (HYSYS v1.2) to check the accuracy of screening models. It is interesting to review Table 7, as it compares (presimulation) energy costs with (postsimulation) rigorous calculations. The synthesis models appear to predict the trends very reliably.

Conventional synthesis representations would typically assign binary variables to represent the number/existence of trays, the location/existence of streams, and/or various interconnections and the existence of individual units. Continuous variables would include mass and energy balances over a superstructure model and would call upon MINLP technology to optimize and solve a particularly difficult system. For the problem at hand, the MINLP model is expected to be challenging and required additional effort to initialize the system and ensure that a not-very-inferior solution is obtained.

Instead, the proposed MILP model only requires binaries for each simple and complex combination of tasks. Specifically, the options include:

- Simple tasks (20 options): A/BCDE, AB/CDE, ABC/DE, ABCD/E, A/BCD, AB/CD, ABC/D, B/CDE, BC/DE, BCD/E, A/BC, AB/C, B/CD, BC/D, C/DE, CD/E, A/B, B/C, C/D, D/E

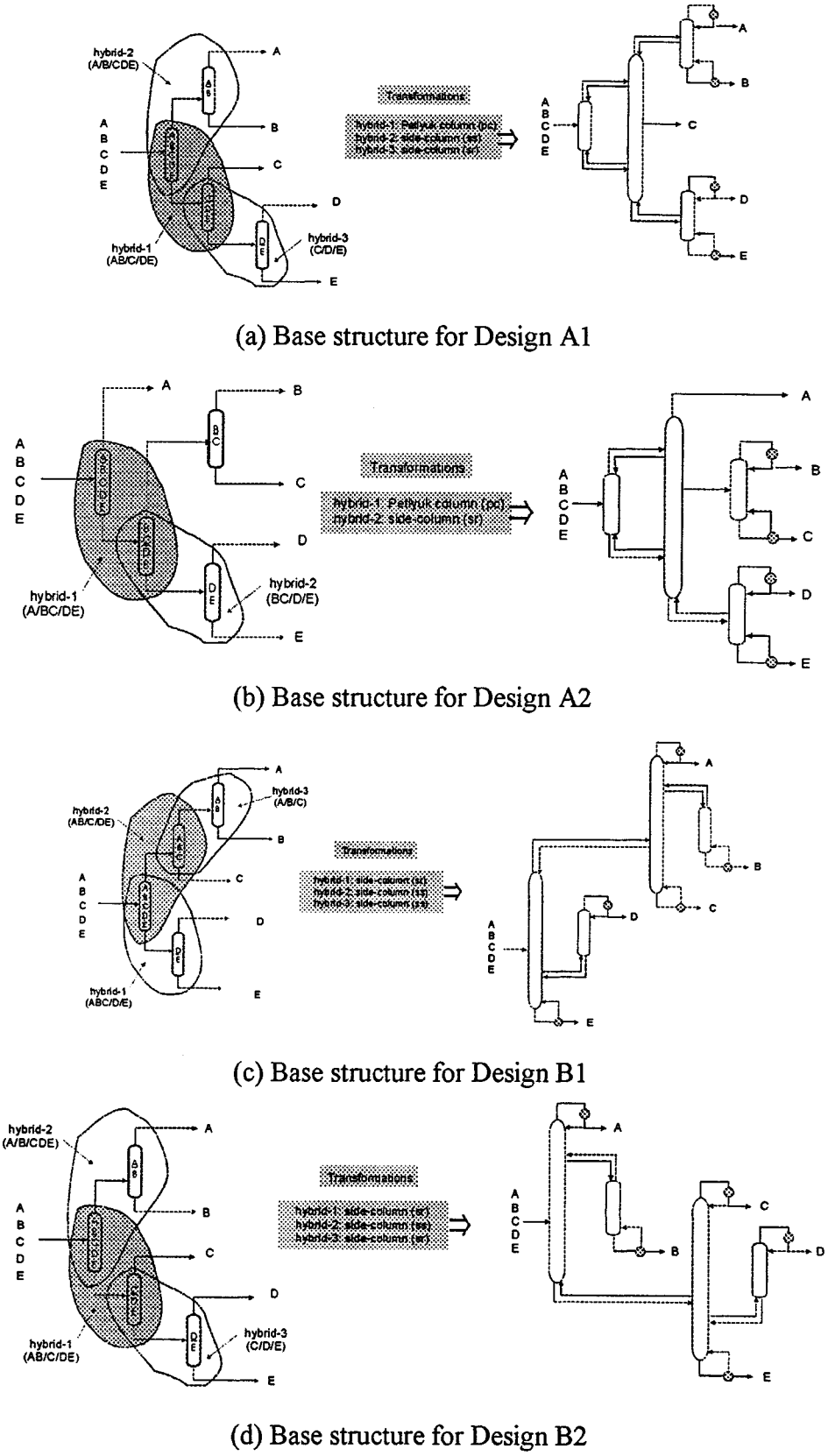

Figure 16. Development of novel designs for Example 5C3.

Table 7. Operating Pressure as a Function of Top Product to Match Specified Cold Utility for Example 4R1

No.	Product Set as Top Product	Cold Utility/ Top Temp. (°C)	Operating Pressure (bar)
1	A	CW, 45	4.84
2	AB	CW, 45	3.22
3	ABC	CW, 45	1.39
4	B	CW. 45	1.71
5	BC	CW, 45	0.77 → 1
6	C	CW, 45	0.55 → 1

- Second-order hybrids (15 options): A/B/CDE, A/BC/DE, A/BCD/E, AB/C/DE, AB/CD/E, ABC/D/E, A/B/CD, A/BC/D, AB/C/D, B/C/DE, B/CD/E, BC/D/E, A/B/C, B/C/D, C/D/E).
- Seven complex transformations for each of the 15 hybrids
- A total of 6 two-feed columns

Because the computational burden is partly delegated for the development of tasks (simple and hybrid), the optimization models are simple and easy to handle. The particular example requires binaries for the performance of the 20 simple columns, the 105 complex column configurations (seven complex transformations for each of the 15 hybrids), and the two-feed columns. The total number of variables is then 131 binary and 20 continuous variables.

Example 4R1: industrial case study

The feed contains nine components of Table 1 and four products: A (C_4 fraction separated as lights), B (iso-pentane and some *n*-pentane), C (C_6 fraction), and D (heavier components, C_7+). The top and bottom products and the available utilities determine the upper and lower limits for the feasible operating pressures (see Tables 7 and 8). The pressure range is uniformly discretized to generate five discrete instances for each task.

Energy cost is used as the synthesis objective. Optimization results are summarized in Figure 17. Designs I to IV represent the favorable four schemes. Design V denotes the best simple sequence. Design I separates the lightest product and uses a prefractionator for the downstream separation in hybrid B/C/D. Design II employs a prefractionator in hybrid AB/C/D to separate plentiful products, C and D, early in the sequence. Design III is similar to Design II with the exception of a side-stripper used instead of the prefractionator in hybrid AB/C/D. Design IV separates the lightest product first and uses a side-stripper (hybrid B/C/D) for the downstream separation. Design V (best simple sequence) separates the plentiful product, D, first and favors difficult separations, B/C, in the end.

Table 8. Operating Pressure as a Function of Bottom Product to Match Specified Hot Utility for Example 4R1

No.	Product Set as Bottom Product	Hot Utility/ Top Temp. (°C)	Operating Pressure (bar)
1	B	MPS, 164	23.01
2	BC	VHP, 210	24.67
3	BCD	VHP, 210	11.98
4	C	VHP, 210	20.95
5	CD	VHP, 210	10.39
6	D	VHP, 210	6.49

Design	Energy Cost	Layout	Column → Pressure (bar)		Trays	Temp.(°C) Top/Bottom	Duty (GJ/h) Top/Bottom
I	6.57	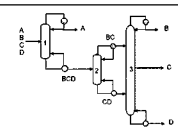	1 →	4.9	30	45.0/153.3	-6.5/9.6
			2 →	1.8	4	74.5/133.2	-3.6/11.6
			3 →	1.8	82	45.0/146.1	-19.8/21.8
		Columns 1: A/BCD; 2,3: pf for B/C/D					
II	6.60	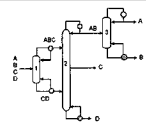	1 →	3.5	4	92.5/163.7	-4.1/5.4
			2 →	3.5	90	51.9/177.7	-22.0/25.1
			3 →	4.9	29	45.0/83.8	-3.3/3.8
		Columns 1,2: pf for AB/C/D; 3: A/B					
III	7.20	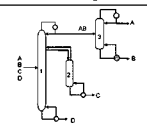	1 →	3.5	37	51.8/177.7	-28.6/26.0
			2 →	3.5	50	---/115.8	---/10.2
			3 →	4.9	29	45.0/83.8	-3.3/3.8
		Columns 1,2: ss for AB/C/D; 3: A/B					
IV	7.50	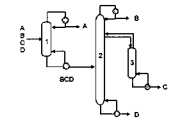	1 →	4.9	30	45.0/153.3	-6.5/9.6
			2 →	1.8	33	46.0/146.1	-27.6/24.3
			3 →	1.8	45	---/88.2	---/9.4
		Columns 1: A/BCD; 2,3: ss for B/C/D					
V	7.60	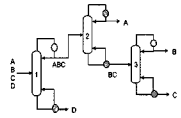	1 →	1.6	23	50.0/136.8	-21.7/26.6
			2 →	4.9	29	45.0/115.1	-4.8/6.3
			3 →	1.8	54	45.0/82.8	-11.1/12.9
		Columns 1: ABC/D; 2: A/BC; 3: B/C					

Figure 17. Promising designs for Example 4R1.

Figure 17 summarizes additional design aspects (operating pressure, temperatures, duties, and so on) useful to initialize rigorous simulation models. Using the cost of Design V as a basis (100 = k$3811/y), designs are reviewed in Table 9. As in the previous illustration, the ranking is identical and the (presimulation) energy costs match very well with the (postsimulation) rigorous costs. Another interesting point is that direct vs. indirect preferences in choice of complex designs do not match with similar choices for simple designs. In this example, the best simple sequence is close to an indirect sequence (Design V), but the best complex scheme corresponds to a direct sequence (Design I).

Table 9. Comparison with the Simulation Results for Example 4R1

No.	Design	Energy Cost (%)	Simulation Energy Cost (%)
1	Design I	86	89
2	Design II	87	91
3	Design III	95	93
4	Design IV	99	96
5	Design V	100	100

Table 10. Problem Specifications for Example 6C1

i	Component	x_i^f	Recovery Fractions in Product A	B	C	D	E	F
1	i-Butane	0.05	0.98	0.02				
2	n-Butane	0.05	0.01	0.98	0.01			
3	Neo-pentane	0.10		0.01	0.98	0.01		
4	n-Pentane	0.15			0.01	0.98	0.01	
5	n-Hexane	0.25				0.01	0.98	0.01
6	n-Heptane	0.40					0.02	0.98
Product fractions: x_i^P			0.049	0.051	0.100	0.150	0.254	0.394
Feed flow rate: F^{tot}			453.6 kmol/h, saturated liquid at 6 bar					

Lowest pressures are selected for all the tasks in the selected designs due to the favorable separation factor (relative volatility). Because of the considerable difference in the operating pressures of associate tasks, designs with extensive thermal coupling are not observed. All complex column configurations require high pressures, and the benefits of thermal coupling are counterbalanced by the requirement of higher reflux. In other words, pressure effects dominate the results and minimize thermal coupling.

Example 6C1: paraffin separation

The paraffin mixture of Table 10 is separated into six products (Porter and Mamoh, 1991). The operating pressure is set to allow cooling water as the coldest utility. The total annualized cost is used as the synthesis objective. The optimization results are summarized in Figure 18. Designs I to III represent the three most promising designs, and Design IV denotes the best simple sequence.

Design I employs two connecting prefractionator arrangements using hybrids ABCD/E/F and AB/C/D (prefractionator transformations). Design II is structurally similar to Design I, except that the second prefractionator distributes products B and C instead of only C. It employs hybrids ABCD/E/F and A/BC/D (prefractionator transformations). Designs I and II separate the plentiful products, E and F, early in the sequence to minimize the load on the downstream separation. Design III distributes C in the first prefractionator, and uses a simple column to perform difficult separation A/B. It employs a second prefractionator for the downstream separation. It uses hybrids A/B/C and D/E/F (prefractionator transformations). Design IV represents the best simple sequence that reserves the difficult split (A/B, B/C) for the end. The complex columns promise up to 17% savings in the total annualized cost against the best simple sequence. Figure 18 summarizes design aspects.

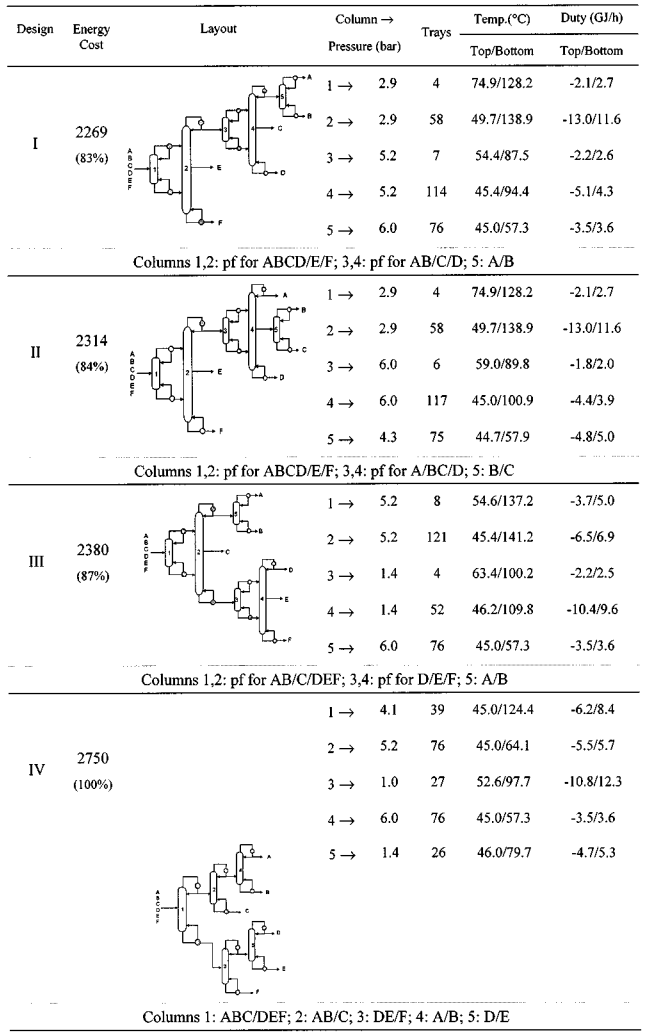

Figure 18. Promising designs for Example 6C1.

Example 8C1: refinery light-end separation

A light-end refinery mixture is fractionated into eight products (Tedder, 1984; Cheng and Liu, 1988). The problem data is presented in Table 11. The feed stream is saturated

Table 11. Problem Specifications for Example 8C1

i	Component	x_i^f	Recovery Fractions in Product A	B	C	D	E	F	G	H
1	22-DMP	0.091	0.98	0.02						
2	i-Pentane	0.169	0.01	0.98	0.01					
3	n-Pentane	0.176		0.01	0.98	0.01				
4	22-DMB	0.019			0.01	0.98	0.01			
5	23-DMB	0.030				0.01	0.98	0.01		
6	2-MP	0.177					0.01	0.98	0.01	
7	n-Hexane	0.112						0.01	0.98	0.01
8	Benzene	0.226							0.02	0.98
Product fractions: x_i^P			0.09	0.17	0.17	0.02	0.03	0.18	0.12	0.22
Feed flow rate: F^{tot}			355.3 kmol/h, saturated liquid at 3 bar							

Design	Energy cost	Layouts	Column →	Pressure (bar)	Trays	Temp.(°C) Top/Bottom	Duty (GJ/h) Top/Bottom
I	23.35 (96%)	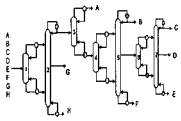	1 →	1.5	9	60.8/88.9	-15.5/18.1
			2 →	1.5	150	49.0/92.3	-46.3/32.2
			3 →	3.1	45	45.5/78.4	-17.6/20.6
			4 →	1.8	7	49.4/72.5	-9.7/10.6
			5 →	1.8	392	44.7/78.9	-84.4/87.2
			6 →	1.4	10	46.5/66.3	-6.7/7.1
			7 →	1.4	150	45.8/68.8	-14.1/9.7
Columns 1,2: pf for ABCDEF/G/H; 3: A/BCDEF; 4,5: pf for B/CDE/F; 6,7: pf for C/D/E							
II	23.76 (98%)	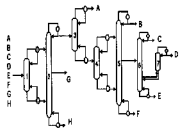	1 →	1.5	9	60.8/88.9	-15.5/18.1
			2 →	1.5	150	49.0/92.3	-46.3/32.2
			3 →	3.1	45	45.5/78.4	-17.6/20.6
			4 →	1.8	7	49.4/72.5	-9.7/10.6
			5 →	1.8	392	44.7/78.9	-84.4/87.2
			6 →	1.4	108	45.8/68.8	-15.0/21.1
			7 →	1.4	35	59.2/---	-4.8/---
Columns 1,2: pf for ABCDEF/G/H; 3: A/BCDEF; 4,5: pf for B/CDE/F; 6,7: sr for C/D/E							
III	23.78 (98%)	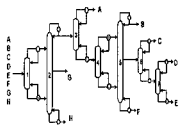	1 →	1.5	9	60.8/88.9	-15.5/18.1
			2 →	1.5	150	49.0/92.3	-46.3/32.2
			3 →	3.1	45	45.5/78.4	-17.6/20.6
			4 →	1.8	7	49.4/72.5	-9.7/10.6
			5 →	1.8	392	44.7/78.9	-84.4/87.2
			6 →	1.4	57	45.9/64.3	-15.0/15.7
			7 →	1.0	86	48.0/57.5	-5.3/5.5
Columns 1,2: pf for ABCDEF/G/H; 3: A/BCDEF; 4,5: pf for B/CDE/F; 6: C/DE; 7: D/E							
IV	24.20 (100%)	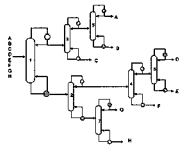	1 →	1.9	58	45.3/87.1	-28.6/33.7
			2 →	1.0	90	58.0/71.9	-42.1/45.6
			3 →	2.2	94	45.0/61.3	-38.5/41.4
			4 →	1.0	289	53.5/59.8	-77.6/80.4
			5 →	3.1	44	45.5/64.4	-11.6/12.7
			6 →	1.0	86	48.0/57.5	-5.3/5.5
			7 →	1.0	49	68.3/79.4	-22.7/23.8
Columns 1: ABC/DEFGH; 2: DEF/GH; 3: AB/C; 4: DE/F; 5: A/B; 6: D/E; 7: G/H							

Figure 19. Promising designs for Example 8C1.

liquid at 3 bar. The operating pressure of tasks is set to allow the use of cooling water as the coldest utility. The total energy cost is used as the synthesis objective. The optimization results are presented in Figure 19. Designs I to III represent the three most promising designs, and Design IV denotes the best simple sequence.

The selected designs emerge as identical structures in the initial development of the sequence, but employ different schemes to separate products C, D, and E. They all use hybrids ABCDEF/G/H and B/CDE/F (prefractionator transformations) and simple task A/BCDEF for the upstream separation. Design I employs a prefractionator (hybrid C/D/E) for the downstream separation. Design II instead uses a side-rectifier in hybrid C/D/E. Design III employs a direct sequence to separate C, D, and E. Design IV favors the balanced split first and reserves the difficult separation, G/H, for the end. The complex schemes favor prefractionators due to their higher separation efficiency. These designs separate plentiful products, G and H, early in the sequence to minimize the mass load on the downstream separations.

Table 12. Problem Specification for Example 3R1

i	Component	x_i^f	Recovery Fractions in Product A	B	C
1	*i*-Butane	0.0490	0.75	0.25	
2	1-Butene	0.5071	0.03	0.95	0.02
3	*n*-Butane	0.0695		0.19	0.81
4	*trans*-2-Butene	0.0946			1.00
5	*cis*-2-Butene	0.2798			1.00
Product fractions: x_i^P			0.052	0.507	0.441
Feed flow rate: F^{tot}			500 kmol/h, saturated liquid at 3 bar		

These designs promise modest savings of about 2–4% against the best simple sequence. The diminishing benefits of thermal coupling are attributed to the adverse effects of pressure constraints.

Example 3R1: separation of C_4 mixture

As a final example, we consider the separation of a close boiling C_4 mixture. The example is an easier problem than the mixtures addressed in the previous cases, and specifications are available from Dunnebier and Pantelides (1999). They are presented in Table 12. The operating pressure of the tasks is fixed and water is used as the cold utility (in the coldest condenser). The total energy cost is used as the synthesis objective. The selected designs are summarized in Figure 20. Designs I to III represent the three most promising designs; Design IV denotes the best simple sequence. Design I employs a Petlyuk column, Design II employs a prefractionator and Design III shows the potential for a three-column sequence that involves the sloppy split in hybrid A/B/C. The intermediate product, B, is also a plentiful product (50%), so promising deigns show a strong preference for the prefractionation of the feed. The indirect sequence (Design IV) is the best simple sequence for this separation. The optimization results of Dunnebier and Pantelides (1999) present the same optimal design, but claim a *need for detailed models*. The new approach presents all potential structures, even with the use of simple MILPs. Solutions of an average performance require a few seconds on a PC notebook.

Conclusions

A new representation is proposed for the synthesis and optimization of complex separation systems. The representation is based on tasks instead of units. The article introduces a new representation that contains an exhaustive superposition of options in the form of a supertask instead of a superstructure representation. The supertask representation is much simpler and easier to optimize. Indeed, the alternative scheme can be formulated as an MILP problem that is possible to solve to global optimality. The approach is illustrated in several problems based on the literature as well as industrial problems. Besides the network complexity they introduced in their models, mathematical programming techniques, in which the current method finds that it belongs, are shown to be unable to defend a record of design innovation. To the contrary, the application of the new approach enables the systematic development of novel layouts and configurations. The

Design	Energy Cost	Layout	Column → Pressure (bar)		Trays	Temp.(°C) Top/Bottom	Duty (GJ/h) Top/Bottom
I	721 (70%)	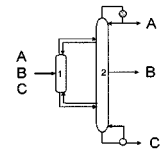	1 →	4.57	35	39.2/45.7	---/---
			2 →	4.57	145	36/49.5	-97/106
	Columns 1,2: pc for A/B/C						
II	756 (73%)	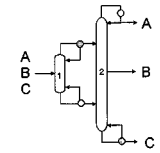	1 →	4.57	35	39.2/45.7	-40/47
			2 →	4.57	138	36/49.5	-65/64
	Columns 1,2: pf for A/B/C						
III	1004 (97%)	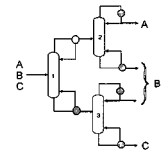	1 →	4.57	35	39.2/47.7	-40/47
			2 →	4.57	63	36/39.8	-41/36
			3 →	4.11	72	36/45.6	-60/63
	Columns 1,2: sp for A/B/C						
IV	1031 (100%)	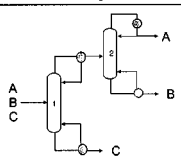	1 →	4.16	77	36/46	85/90
			2 →	4.57	83	36/39,8	59/61
	Columns 1: AB/C; 2: A/B						

Figure 20. Promising designs for Example 3R1.

reader is encouraged to review the designs shown in Figure 15, Figure 17, Figure 18, Figure 19, and Figure 20. They all contain novel designs that are obtained with the new approach. In most cases, the presented results surprised experts in the field, who expected other solutions to be optimal.

A large number of industrial studies have been used to test and validate the research. In most cases, the results have produced new ideas or significantly reduced the time for process analysis. To assess the advantages of the supertask representation, the authors encourage comparisons with tools based on superstructures. Developments are presented for zeotropic mixtures, but there is no limitation to the property models that can be used. Because the optimization requires minimum effort, the approach is particularly useful as a screening tool to consult on favorable designs and integrated layouts. Overall, the article produces strong evidence that tasks are more appropriate to synthesize than units. In this context, the article stands as an argument against expectations that the superstructures will eventually take over the synthesis effort. The idea of using tasks extends beyond pure distillation processes. At a minimum, tasks can accommodate other equilibrium-based methods. The authors expect, however, that the approach will eventually prove appropriate for more general applications.

Acknowledgment

The authors acknowledge financial support from the Process Integration Research Consortium at the University of Manchester Institute of Science and Technology, United Kingdom. A large number of industrial studies have been made possible with the collaboration of M. W. Kellogg, Esso, Aspen Tech, Hyprotech, and UOP.

Notation

a^{ann} = annualization factor
b = bottoms flow rate
C = set of transformations of hybrid
C^{dir} = set of transformations attached to direct associate sequence
C^{ind} = set of transformations attached to indirect associate sequence
C_h = set of hybrid and transformation combinations
C^{cold} = cold utility cost index
$Cost^{\text{energy}}$ = energy cost
$Cost^{\text{tot}}$ = total cost
d = distillate flow rate
$E_{u,p}$ = parameter describing the specified objective of $u \in U$ in $p \in P$
f = feed flow rate of a task
F = nominal feed flow rate of a task
F^{tot} = total feed flow rate
G = set of multiple-feed columns
G_h^{slp} = set of multiple-feed columns attached to sloppy split transformation of $h \in H$
H = set of hybrids
H_t^{asso} = set of hybrids attached to associate task $t \in T$
I = set of component in feed
L = liquid flow rate
L_u^{opc} = maximum discrete instances of $u \in U$
$L_{t,c}^{\text{hyb}}$ = maximum number of $c \in C$ attached to all hybrids of $t \in T$
L_h^{ovl} = maximum transformations of $h \in H$
L_c^{tra} = overall maximum number of transformations, $c \in C$
M = set of product subgroups
N = set of products
NT = number of trays
P = set of discrete instances
q = feed quality
Q^{cond} = condenser duty
Q^{reb} = reboiler duty
R^{MIN} = minimum reflux
RF = ratio of actual reflux to the minimum reflux
$S_{u,p}$ = design discounts in $E_{u,p}$ employing $u \in C_h$, $p \in P$
SS = number of product subgroups
SQ = number of simple sequences
T = set of simple task
T_m^{out} = set of tasks producing $m \in M$
T_m^{inp} = set of tasks receiving $m \in M$
T_h^{dir} = set of tasks in the direct associate sequence of $h \in H$
T_h^{ind} = set of tasks in the indirect associate sequence of $h \in H$
T_g^{mfd} = set of tasks producing same products with $g \in G$
T^{fr} = set of tasks receiving fresh feed
T^{int} = set of tasks receiving intermediate feed
U = set of all tasks, $T \cup C_h$
V = vapor load
w = side-draw flow rate
x_i^b = bottom product composition
x_i^d = distillate product composition
x_i^f = feed composition
y = composition in the vapor phase
Y = binary variable for the existence of task

Greek letters

α_i = relative volatility
θ = root(s) of Underwood equation
$\zeta_{m,t}$ = fraction of feed that yields stream $m \in M$

Indices

b = bottoms
c = transformation, $c \in C$
d = distillate

h = hybrid, $h \in H$
i = component, $i \in I$
p = discrete instance, $p \in P$
t = discrete instance, $t \in T$
u = basic task, $u \in U$
w = side draw

General

HC = heavy components
HK1 = heavy key for the lighter split of hybrid
HK2 = heavy key for the heavier split of hybrid
HP = heavy product
I, II, III, IV = columns in the equivalent arrangements of the complex columns
IC = intermediate components
IP = intermediate product
LC = light components
LK1 = light key for lighter split of hybrid
LK2 = light key for heavier split of hybrid
LP = light product
pc = Petlyuk column transformation
pf = prefractionator transformation
sl = liquid side-draw transformation
sp = sloppy split transformation
sr = side-rectifier transformation
ss = side-stripper transformation
sv = vapor side-draw transformation

Literature Cited

Agrawal, A., and C. A. Floudas, "Synthesis of Heat Integrated Nonsharp Distillation Sequences," *Comput. Chem. Eng.*, **16**, 89 (1992).

Agrawal, R., and Z. Fidkowski, "More Operable Arrangements of Fully Thermally Coupled Distillation Columns," *AIChE J.*, **44**, 2565 (1998).

Agrawal, R., "Synthesis of Distillation Column Configurations for a Multicomponent Separation," *Ind. Eng. Chem. Res.*, **35**, 1059 (1996).

Bauer, M. H., and J. Stichlmair, "Superstructures for the Mixed Integer Optimisation of Nonideal and Azeotropic Distillation Processes," *Comput. Chem. Eng.*, **20**, S25 (1997).

Bausa, J., R. V. Watzdorf, and W. Marquardt, "Shortcut Methods for Nonideal Multicomponent Distillation: 1. Simple Columns," *AIChE J.*, **44**, 2181 (1998).

Brooke, K. E., D. Kendrick, and A. Meeraus, *GAMS: A Users Guide*, Scientific Press, San Francisco, CA (1988).

Caballero, J. A., and I. E. Grossmann, "Aggregated Models for Integrated Distillation Systems," *Ind. Eng. Chem. Res.*, **38**, 2330 (1999).

Carlberg, N. A., and A. W. Westerberg, "Temperature-Heat Diagrams for Complex Columns. 2. Underwood's Method for Side Strippers and Enrichers," *Ind. Eng. Chem. Res.*, **28**, 1379 (1989a).

Carlberg, N. A., and A. W. Westerberg, "Temperature-Heat Diagrams for Complex Columns. 3. Underwood's Method for the Petlyuk Configuration," *Ind. Eng. Chem. Res.*, **28**, 1386 (1989b).

Cheng, S. H., and Y. A. Liu, "Studies in Chemical Process Design and Synthesis. 8. A Simple Heuristic Method for the Synthesis of Initial Sequences for Sloppy Multicomponent Separations," *Ind. Eng. Chem. Res.*, **27**, 2304 (1988).

Christiansen, A. C., S. Skogestad, and K. Lein, "Complex Distillation Arrangements: Extending Their Ideas," *Comput. Chem. Eng.*, **21**, S237 (1997).

Douglas, J. M., *Conceptual Design of Processes*, McGraw-Hill, New York (1988).

Dunnebier, G., and C. C. Pantelides, "Optimal Design of Thermally Coupled Distillation Columns," *Ind. Eng. Chem. Res.*, **38**, 162 (1999).

Fidkowski, Z., and L. Krolikowski, "Thermally Coupled System of Distillation Columns: Optimisation Procedure," *AIChE J.*, **32**, 537 (1986).

Fidkowski, Z., and L. Krolikowski, "Minimum Energy Requirements of Thermally Coupled Distillation Systems," *AIChE J.*, **33**, 643 (1987).

Fidkowski, Z., and L. Krolikowski, "Energy Requirements of Nonconventional Distillation Systems," *AIChE J.*, **36**, 1275 (1990).

Floudas, C. A., and G. E. Paules IV, "A MINLP Formulation for the Synthesis of Heat Integrated Distillation Sequences," *Comput. Chem. Eng.*, **12**, 531 (1988).

Flowers, T. L., B. K. Harrison, and M. J. Niccolai, "Automated Synthesis of Distillation Sequences Using Fuzzy Logic and Heuristics," *AIChE J.*, **40**, 1341 (1994).

Glanz, S., and J. Stichlmair, "Minimum Energy Demand of Distillation Columns with Multiple Feeds," *Chem. Eng. Technol.*, **20**, 93 (1997).

Glinos, K., and M. F. Malone, "Minimum Reflux, Product Distribution, and Lumping Rules for Multi-Component Distillation," *Ind. Eng. Chem. Process Des. Dev.*, **23**, 764 (1984).

Glinos, K., and M. F. Malone, "Design of Side-Stream Distillation Columns," *Ind. Eng. Chem. Process Des. Dev.*, **24**, 822 (1985).

Glinos, K., and M. F. Malone, "Optimality Regions for Complex Column Alternatives in Distillation Systems," *Chem. Eng. Res. Des.*, **66**, 229 (1988).

Hendry, J. E., and R. R. Hughes, "Generating Separation Process Flowsheets," *Chem. Eng. Prog.*, **68**, 71 (1972).

Ismail, S. R., E. N. Pistikopoulos, and K. P. Papalexandri, "Modular Representation Synthesis Framework for Homogeneous Azeotropic Separation," *AIChE J.*, **45**, 1701 (1999).

Kaibel, G., "Distillation Columns with Vertical Partitions," *Chem. Eng. Technol.*, **10**, 92 (1987).

Kaibel, G., "Distillation Column Arrangements with Low Energy Consumption," *Inst. Chem. Eng. Symp. Ser.*, **109**, 43 (1988).

Kaibel, G., E. Blass, and J. Kohler, "Thermodynamics-Guideline for the Development of Distillation Column Arrangements," *Gas Sep. Purif.*, **4**, 109 (1989).

Koehler, J., P. Aguirre, and E. Blass, "Evolutionary Thermodynamic Synthesis of Zeotropic Distillation Sequences," *Gas Sep. Purif.* **6**, 153 (1992).

Nikolaides, I. P., and M. F. Malone, "Approximate Design of Multiple-Feed/Side-Stream Distillation Systems," *Ind. Eng. Chem. Res.*, **26**, 1839 (1987).

Nikolaides, I. P., and M. F. Malone, "Approximate Design and Optimisation of a Thermally Coupled Distillation with Prefractionation," *Ind. Eng. Chem. Res.*, **27**, 811 (1988).

Papaexandri, K. P., and E. N. Pistikopoulos, "Generalized Modular Representation Framework for Process Synthesis," *AIChE J.*, **42**, 1010 (1996).

Petlyuk, F. B., V. M. Platonov, and D. M. Slavinskii, "Thermodynamically Optimal Method for Separating Multicomponent Mixtures," *Int. Chem. Eng.*, **5**, 555 (1965).

Porter, K. E., and S. O. Mamoh, "Finding the Optimum Sequence of Distillation Columns—An Equation to Replace the Rule of Thumb," *Chem. Eng.*, **46**, 97 (1991).

Sargent, R. W. H., and K. Gaminibandara, "Optimum Design of Plate Distillation Columns," *Optimisation in Action*, L. C. W. Dixon, ed., Academic Press, London, p. 267 (1976).

Sargent, R. W. H., "Functional Approach to Process Synthesis and its Application to Distillation Systems," *Comput. Chem. Eng.*, **22**, 31 (1998).

Smith, E. M. B., and C. C. Pantelides, "Design of Reaction Separation Networks Using Detailed Models," *Comput. Chem. Eng.*, **19**, S83 (1995).

Stichlmair, J., "Distillation and Rectification," *Ullmann's Encyclopedia of Industrial Chemistry*, Vol. B3, p. 4.1 (1988).

Stupin, W. J., and F. J. Lockhart, "Thermally Coupled Distillation—A Case History," *Chem. Eng. Prog.*, **68**, 71 (1972).

Tedder, D. W., and D. F. Rudd, "Parametric Studies in Industrial Distillation," *AIChE J.*, **24**, 303 (1978).

Tedeer, D. W., "The Synthesis of Optimal Gas Saturates Separation System," AIChE Meeting, San Francisco, CA (1984).

Triantafyllou, C., "The Design, Optimisation and Integration of Dividing Wall Columns," PhD Thesis, Univ. of Manchester Institute of Science and Technology, UK (1991).

Triantafyllou, C., and R. Smith, "The Design and Optimisation of Fully Thermally Coupled Distillation Columns," *Trans. Inst. Chem. Eng.*, **70**, 118 (1992).

Wankat, P. C., *Equilibrium Staged Operations*, Elsevier, New York (1988).

Yeomans, H., and I. E. Grossmann, "Disjunctive Programming Models for the Optimal Design of Distillation Columns and Separation Sequences," *Ind. Eng. Chem. Res.*, **39**, 1637 (2000a).
Yeomans, H., and I. E. Grossmann, "Optimal Design of Complex Distillation Columns Using Rigorous Tray-by-Tray Disjunctive Programming Models," *Ind. Eng. Chem. Res.*, **39**, 4326 (2000b).

Appendix: Shortcut Models for Complex Distillation Arrangements

The modeling elements involved in various configurations of the complex columns representing different transformations were presented in the fourth section. This Appendix describes the governing equations for the complex arrangements. The first section below presents the procedure for calculating the optimum recovery of the ICs in the distillate of the prefractionator. The detailed model with all the necessary equations for the thermally coupled prefractionator design is presented in the second section. The Fenske–Gilliland equation for the calculation of the number of theoretical stages is presented in the third section. The shortcut model for the two-feed columns is described with all necessary equations and finally, the simplified model for the side-draw columns is presented.

Performance of prefractionator

In the prefractionator column, the first light key (LK1) is separated from the second heavy key (HK2), and all the components of intermediate products are distributed between its top and the bottom products. The recovery of the ICs in the distillate of the prefractionator is a degree of freedom, and it is varied to minimize the reflux requirement in the prefractionator. The optimum recovery of the ICs is calculated by solving two parts of the Underwood equation simultaneously. The first part of the Underwood equation (Eq. A1) is written for the feed composition and solved to obtain a root for each pair of key and intermediate components

$$\sum_{i \in 1} \frac{x_i^{f,\mathrm{I}} \cdot \alpha_i}{\alpha_i - \theta_j^I} = 1 - q^{\mathrm{I}} \quad \forall\, j \in J \tag{A1}$$

where $j \in J$ represents the pairs of components involved in the prefractionation. θ_j is the root of the Underwood equation, such that its value lies between the relative volatilities of the component forming the pair j, that is $\alpha_{i+1} < \theta_j < \alpha_i$.

The values of θ_j are used in the second part of the Underwood equation (Eq. A2) along with the mole-fraction summation constraint (Eq. A3) and the product specifications constraints (Eqs. A4 to A7) to obtain the distillate composition

$$\sum_{i \in \mathrm{I}} \frac{y_i^{d,\mathrm{I}} \cdot \alpha_i}{\alpha_i - \theta_j^{\mathrm{I}}} = R^{\mathrm{MIN},I} + 1 \qquad \forall\, j \in J \tag{A2}$$

$$\sum_{i \in \mathrm{I}} y_i^{d,\mathrm{I}} = 1 \tag{A3}$$

$$y_i^{d,\mathrm{I}} \cdot d^{\mathrm{I}} = \Re_i^{d,\mathrm{I}} \cdot x_i^{f,\mathrm{I}} \cdot f^{\mathrm{I}} \qquad \forall\, i = \mathrm{LK1} \tag{A4}$$

$$y_i^{d,\mathrm{I}} \cdot d^{\mathrm{I}} = x_i^{f,\mathrm{I}} \cdot f^{\mathrm{I}} \qquad \forall\, i \in \text{lighter than LK1} \tag{A5}$$

$$y_i^{d,\mathrm{I}} \cdot d^{\mathrm{I}} = \left(1 - \Re_i^{b,\mathrm{I}}\right) \cdot x_i^{f,\mathrm{I}} \cdot f^{\mathrm{I}} \qquad \forall\, i = \mathrm{HK2} \tag{A6}$$

$$y_i^{d,\mathrm{I}} = 0 \qquad \forall\, i \in \text{heavier than HK2} \tag{A7}$$

In the Column I, the LK1 recovery in distillate ($\Re_{\mathrm{LK1}}^{d,\mathrm{I}}$) and HK2 in bottoms ($\Re_{\mathrm{HK2}}^{b,\mathrm{I}}$) is calculated from the product specifications. In this model, the number of variables is the same as the number of independent equations. The presented set of equations (A2 to A7) is solved simultaneously to obtain distillate composition, flow rate, and the minimum reflux ratio. The bottom product composition and flow rate are then calculated using material-balance equations. The model represents the system completely and provides optimum recovery of IC in the first column. In this way, the nature of the problem is used to optimize the recovery of the ICs in the prefractionator.

Petlyuk column design

The performance of the prefractionator is predicted using the shortcut model presented in the previous section. The net distillate and bottom-product composition and flow rates of the prefractionator are exploited to calculate the actual composition and flow rates of the feed and side-draw streams of Columns II and III. Note that the Column II feed is vapor, while that of Column III is liquid. Similarly, the side-draw of Column II is liquid and Column III is vapor. Equations describing a flash calculation for the partial condenser and reboiler are

$$f^{\mathrm{II}} = \left(R^{\mathrm{MIN,I}} \cdot RF + 1\right) \cdot d^{\mathrm{I}} \tag{A8}$$

$$w^{\mathrm{II}} = R^{\mathrm{MIN,I}} \cdot RF \cdot d^{\mathrm{I}} \tag{A9}$$

$$x_i^{w,\mathrm{II}} = \frac{y_i^{d,\mathrm{I}}/\alpha_i}{\sum_{k \in \mathrm{I}} y_k^{d,\mathrm{I}}/\alpha_k} \tag{A10}$$

$$y_i^{f,\mathrm{II}} = \frac{y_i^{d,\mathrm{I}} \cdot d^{\mathrm{I}} + x_i^{w,\mathrm{II}} \cdot w^{\mathrm{II}}}{d^{\mathrm{I}} + w^{\mathrm{II}}} \tag{A11}$$

$$f^{\mathrm{III}} = R^{\mathrm{MIN,I}} \cdot RF \cdot d^{\mathrm{I}} + q^{\mathrm{I}} \cdot f^{\mathrm{I}} \tag{A12}$$

$$w^{\mathrm{III}} = \left(R^{\mathrm{MIN,I}} \cdot RF + 1\right) \cdot d^{\mathrm{I}} - \left(1 - q^{\mathrm{I}}\right) \cdot f^{\mathrm{I}} \tag{A13}$$

$$y_i^{w,\mathrm{III}} = \frac{x_i^{b,\mathrm{I}} \cdot \alpha_i}{\sum_{k \in I} x_k^{b,\mathrm{I}} \cdot \alpha_k} \tag{A14}$$

$$x_i^{f,\mathrm{III}} = \frac{x_i^{b,\mathrm{I}} \cdot b^{\mathrm{I}} + y_i^{w,\mathrm{III}} \cdot w^{\mathrm{III}}}{d^{\mathrm{I}} + w^{\mathrm{III}}} \tag{A15}$$

These compositions are now used to estimate vapor–liquid traffic in Column II and Column III using Underwood's equation for the towers with side-draw.

The feed to Column II is saturated vapor (that is, $q^{\mathrm{II}} = 0$), and it performs the lighter split, hence the root of Underwood's equation, θ^{II}, should be between the relative volatility of LK1 and HK1. The minimum reflux ratio is then calculated for the column by assuming a liquid side-draw, w^{II}, from the rectifying section of the column using the second part of

Underwood's equation (Eq. A17)

$$\sum_{i \in \mathrm{I}} \frac{y_i^{f,\mathrm{II}} \cdot \alpha_i}{\alpha_i - \theta^{\mathrm{II}}} = 1 \qquad \alpha_{\mathrm{HK1}} < \theta^{\mathrm{II}} < \alpha_{\mathrm{LK1}} \tag{A16}$$

$$\sum_{i \in \mathrm{I}} \frac{\left(x_i^{d,\mathrm{II}} + \left\{w^{\mathrm{II}}/d^{\mathrm{II}}\right\} \cdot x_i^{w,\mathrm{II}}\right) \cdot \alpha_i}{\alpha_i \cdot \theta^{\mathrm{II}}} = R^{\mathrm{MIN,II}} + 1. \tag{A17}$$

The feed to Column III is saturated liquid (that is, $q^{\mathrm{III}} = 1$), and it performs the heavier split, hence the root of Underwood's equation, θ^{III}, should be between the relative volatility of LK2 and HK2. The minimum reflux ratio is then calculated for the column by assuming a vapor side-draw, w^{III}, from the stripping section of the column using the second part of Underwood's equation (Eq. A19)

$$\sum_{i \in \mathrm{I}} \frac{x_i^{f,\mathrm{III}} \cdot \alpha_i}{\alpha_i - \theta^{\mathrm{III}}} = 0 \qquad \alpha_{\mathrm{HK2}} < \theta^{\mathrm{III}} < \alpha_{\mathrm{LK2}} \tag{A18}$$

$$-\sum_{i \in \mathrm{I}} \frac{\left(\left\{b^{\mathrm{III}}/d^{\mathrm{III}}\right\} \cdot x_i^{b,\mathrm{III}} + \left\{w^{\mathrm{III}}/d^{\mathrm{III}}\right\} \cdot y_i^{w,\mathrm{III}}\right) \cdot \alpha_i}{\alpha_i - \theta^{\mathrm{III}}} = R^{\mathrm{MIN,III}} + 1 \tag{A19}$$

The information about the reflux ratio, feed and product streams, and side-draws is used in a simple material-balance equation of each section of the column to obtain extact vapor and liquid traffic. General expressions for vapor-liquid flow rates (in the column with the liquid side-draw from the rectifying section and/or vapor side-draw from stripping section) are presented below

$$V^{\mathrm{rect}} = \left(R^{\mathrm{MIN}} \cdot RF + 1\right) \cdot d \tag{A20}$$

$$V^{\mathrm{strp}} = V^{\mathrm{rect}} - (1 - q) \cdot f + \sum_{\substack{\text{vapor} \\ \text{side-draw}}} w \tag{A21}$$

$$L^{\mathrm{rect}} = R^{\mathrm{MIN}} \cdot RF \cdot d \tag{A22}$$

$$L^{\mathrm{strp}} = L^{\mathrm{rect}} + q \cdot f - \sum_{\substack{\text{liquid} \\ \text{side-draw}}} w \tag{A23}$$

In the Petlyuk column, thermal coupling between Columns II and III is performed, hence it is necessary to equalize vapor-liquid traffic in the bottom of Column II with the top of Column III. This is done by choosing the higher of the two, and thus operating one column at a higher reflux than 1.1 times R^{MIN}. A detailed explanation of the presented model can be found in Triantafyllou and Smith (1992).

The equivalent arrangements of the side-column and the prefractionator arrangements can be treated as the specific cases of the presented model. For example, when recovery of the IC in the distillate of Column I is forced to 1, the model represents a side-stripper arrangement. If it is 0, a side-rectifier arrangement is realized. The exact equations for the calculation of the design parameters are obtained easily by adapting the presented model.

Calculation of the number of stages

The relative volatility and recovery fractions of the key components are used in the Fenske equation (Eq. A24) to calculate the minimum number of theoretical stages. The actual number of theoretical stages required for the desired separation when the column is operated at 1.1 times R^{MIN} (that is, $RF = 1.1$) is calculated using Gilliland's equation (Eq. A25). The feed-tray location is estimated using Kirkbride's correlation (Eq. A26). The expressions of this shortcut model are presented below

$$N^{\mathrm{MIN}} = \frac{LN\left[\left(x_{LK}^d/x_{HK}^d\right) \cdot \left(x_{HK}^b/x_{LK}^b\right)\right]}{LN\left[\alpha_{LK}/\alpha_{HK}\right]} \tag{A24}$$

$$\frac{NT - N^{\mathrm{MIN}}}{NT + 1} = 1 - \exp\left(\frac{1 + 54.4 \cdot \aleph}{11 + 117.2 \cdot \aleph} \cdot \frac{\aleph - 1}{\aleph^{0.5}}\right) \tag{A25}$$

where

$$\aleph = \frac{RF - 1}{RF + \dfrac{1}{R^{\mathrm{MIN}}}}$$

$$\frac{NT^{\text{above feed}}}{NT - NT^{\text{above feed}}} = \left[\frac{x_{HK}^f}{x_{LK}^f} \cdot \left(\frac{x_{LK}^b}{x_{HK}^d}\right)^2 \cdot \frac{b}{d}\right]^{0.206} \tag{A26}$$

The presented shortcut model for calculating the number of stages is used for Columns II and III with appropriate modifications. The Fenske equation is applied to these columns above and below the side-draw, as shown in Eqs. A27 and A28 respectively. The Gilliland's correlation is then used in an exactly identical manner to obtain the actual number of stages in each section of the column.

$$N^{\mathrm{MIN},\substack{\text{above}\\ \text{side-draw}}} = \frac{LN\left[\left(x_{LK}^d/x_{HK}^d\right) \cdot \left(x_{HK}^w/x_{LK}^w\right)\right]}{LN\left[\alpha_{LK}/\alpha_{HK}\right]} \tag{A27}$$

$$N^{\mathrm{MIN},\substack{\text{below}\\ \text{side-draw}}} = \frac{LN\left[\left(x_{LK}^w/x_{HK}^w\right) \cdot \left(x_{HK}^b/x_{LK}^b\right)\right]}{LN\left[\alpha_{LK}/\alpha_{HK}\right]} \tag{A28}$$

Multiple-feed columns

The two-feed column is decomposed into two hypothetical simple columns, each receiving one feed. The top product of Column IV-1 and the bottom product of Column IV-2 represent the distillate and bottom products of the actual column respectively. The pseudobottom product of Column IV-1 is obtained by subtracting the lower feed (f_2) from the overall bottom product (b), while the pseudotop product of Column IV-2 is calculated by subtracting the upper feed (f_1) from the overall distillate product (d). These two pseudoproducts are always in equal magnitude and opposite direction. For the desired split, the first part of the Underwood equation is used separately in both hypothetical simple columns to calculate

the two θ values associated with them (see Eqs. A29 and A30)

$$\sum_{i \in \mathrm{I}} \frac{x_i^{f,\mathrm{IV}-1} \cdot \alpha_i}{\alpha_i - \theta^{\mathrm{IV}-1}} = 1 - q^{\mathrm{IV}-1} \tag{A29}$$

$$\sum_{i \in \mathrm{I}} \frac{x_i^{f,\mathrm{IV}-2} \cdot \alpha_i}{\alpha_i - \theta^{\mathrm{IV}-2}} = 1 - q^{\mathrm{IV}-2} \tag{A30}$$

These θ values are then used in the second part of the Underwood equation (see Eqs. A31 and A32) to predict the pseudoreflux ratio ($r^{\min}$) in the rectifying section of both the hypothetical columns.

$$\sum_{i \in \mathrm{I}} \frac{x_i^{d,\mathrm{IV}} \cdot \alpha_i}{\alpha_i - \theta^{\mathrm{IV}-1}} = r^{\min,\mathrm{IV}-1} + 1 \tag{A31}$$

$$\sum_{i \in \mathrm{I}} \frac{\left(\dfrac{d^{\mathrm{IV}} \cdot x_i^{d,\mathrm{IV}} - f^{\mathrm{IV}-1} \cdot x_i^{f,\mathrm{IV}-1}}{d^{\mathrm{IV}} - f^{\mathrm{IV}-1}} \right) \cdot \alpha_i}{\alpha_i - \theta^{\mathrm{IV}-2}} = r^{\min,\mathrm{IV}-2} + 1 \tag{A32}$$

The pseudoreflux ratios are used to predict the actual reflux ratio (R^{MIN}) in the two-feed column. When the upper feed is controlling, the pseudoreflux ratio of the first column (Column IV-1) is the same as the actual reflux ratio of the column. The actual reflux ratio of the column when the lower feed is controlling is calculated using the pseudoreflux ratio of the second column (Column IV-2), and the balance equation for the liquid flow between the two hypothetical columns is shown below

$$R^{\mathrm{MIN},\mathrm{IV}-1} = r^{\min,\mathrm{IV}-1} \tag{A33}$$

$$R^{\mathrm{MIN},\mathrm{IV}2} = r^{\min,\mathrm{IV}-2} \cdot \left(1 - \frac{f^{\mathrm{IV}-1}}{d^{\mathrm{IV}}}\right) - \frac{f^{\mathrm{IV}-1}}{d^{\mathrm{IV}}} \cdot q^{\mathrm{IV}-1} \tag{A34}$$

The two values of the actual reflux ratio are then compared to decide the controlling feed. The higher of two reflux values is selected for the operation of the column

$$R^{\mathrm{MIN},\mathrm{IV}} = \max(R^{\mathrm{MIN},\mathrm{IV}-1}, R^{\mathrm{MIN},\mathrm{IV}-2}) \tag{A35}$$

The number of theoretical stages in the multiple-feed column is the same as that in the corresponding simple column, as both the columns have the same product recovery specifications. A detailed discussion of the presented model and its extension to multiple-feed columns is presented in Nikolaides and Malone (1987). A more accurate model for the evaluation of multiple-feed columns can be found in Glanz and Stichlmair (1997).

Side-draw columns

The side-draw columns primarily perform a leading split and effectively use available vapor-liquid in the supplementary column section to carry out further separation. It has a smaller number of column sections, hence it is not possible to achieve any degree of separation without excessive reflux penalty. In this section, the shortcut model of Glinos and Malone (1985) is summarized to identify the feasibility of the side-draw column.

Vapor Side-Draw Column. The first associate task of the direct pair represents the leading split for the vapor side-draw column. The liquid from Column I is used in the supplementary section (Section II) to separate IP from HP. Only a limited degree of separation between IP and HP is possible, as only one column section is available. The LP is obtained as the distillate of the column at the specified purity and recovery in this configuration. Because the separation between IP and HP is imperfect, a fraction of HP gets carried over to side-draw and some amount of IP goes in the bottom product.

The objective of this shortcut model is to predict the minimum fraction of all heavy components (HC) in the vapor side-draw when the reflux ratio is fixed. It is assumed that the flow rate of the side-draw (w) and the bottom product (b) are known from the fractions of IP and HP in the feed stream, respectively. This information is used with the vapor-liquid traffic of the column representing the leading split to predict the boilup ratio in the supplementary stripping section

$$V^{\mathrm{II}} = V^{\mathrm{I}} + w \tag{A36}$$

$$L^{\mathrm{II}} = L^{\mathrm{I}} \tag{A37}$$

$$B = \frac{V^{\mathrm{II}}}{b} \tag{A38}$$

The boilup ratio of the supplementary section can be used with the Underwood equation to calculate the composition of the vapor side-draw. The limiting fraction of HC in the side-draw is the pinch composition under the condition of limiting boilup and the infinite trays in the supplementary stripping section. It can be obtained using the following equation:

$$(y_i^w)_{\min} = \frac{1}{B \cdot (\alpha_{LK2-i} - 1)} \quad \forall\, i \in \mathrm{HC} \tag{A39}$$

The mass-balance equations are then used to predict the composition of IP in the bottoms. Instead of fixing the flow rate of the side-draw and bottoms product, recovery or purity specifications on the bottom product can be used in an exactly identical way to predict the side-draw composition. A detailed discussion and the underlying logic of this model can be found in Glinos and Malone (1985).

Liquid Side-Draw Column. The first associate task of the indirect pair represents the leading split for the liquid side-draw column. The vapor of Column I is used in the supplementary section (Section II) to separate IP from LP. Only a limited degree of separation between LP and IP is possible, as only one column section is available. The HP is obtained as the bottom product of the column at the specified purity and recovery in this configuration. Because the separation

between LP and IP is imperfect, a fraction of LP gets carried over to the side-draw and some amount of IP goes in the distillate.

The objective of this shortcut model is to predict the minimum fraction of all light components (LC) in the liquid side stream when the boilup ratio is fixed. It is assumed that the flow rate of the side-draw (w) and the distillate (d) are known from the fractions of IP and LP in the feed stream, respectively. This information is used with the vapor–liquid traffic of the column representing a leading split to predict the reflux ratio in the supplementary rectifying section

$$V^{\mathrm{II}} = V^{\mathrm{I}} \tag{A40}$$

$$L^{\mathrm{II}} = L^{\mathrm{I}} + w \tag{A41}$$

$$R = \frac{L^{\mathrm{II}}}{d} \tag{A42}$$

The reflux ratio of the supplementary section can be used with the Underwood equation to calculate the composition of the liquid side-draw. The limiting fraction of LC in the side-draw is the pinch composition under the limiting reflux condition and the infinite trays in the supplementary rectifying section. It can be obtained using the following equation

$$(x_i^w)_{\min} = \frac{x_i^d}{R \cdot (\alpha_{i-HK1} - 1)} \quad \forall\, i \in \mathrm{LC} \tag{A43}$$

The mass-balance equations are then used to predict the composition of IP in the distillate. Instead of fixing the flow rate of the side-draw and distillate, recovery or purity specifications on the distillate product can be used in an identical way to predict the side-draw composition. A detailed discussion and the underlying logic of this model can be found in Glinos and Malone (1985).

Manuscript received Aug. 9, 1999, and revision received July 6, 2001.